BIOMEDICAL RESEARCH INSTITUTE (BRI)

FOUNDATION FOR RESEARCH AND TECHNOLOGY HELLAS (FORTH)

UNIVERSITY OF IOANNINA

FACULTY OF MEDICINE

Master's Thesis:

Role of matrix stiffness in lung cancer cell response to treatment

Inter-institutional Interdepartmental Program of Postgraduate Studies "Molecular – Cellular Biology and Biotechnology"

Supervisor: Assistant Prof. Maria Georgiadou

Nektarios Petropoulos

Ioannina, 2026

Acknowledgements

This thesis was conducted at the Biomedical Research Institute (BRI) – Foundation for Research and Technology Hellas (FORTH).

First and foremost, I would like to express my deepest gratitude to my principal investigator, Ms. Maria Georgiadou, Assistant Professor of Cellular Biology, for providing me with the opportunity to undertake this research. Her invaluable guidance, encouragement, and support throughout this journey have been instrumental in shaping this thesis and my academic growth.

I am also very thankful to Professor Eustathios Frilingos, Assistant Professor Dimitris Liakopoulos, Professor Evangelos Kolettas, and Associate Professor Dimitris Beis for being on my master's thesis examination committee.

I am also deeply grateful to Dr. Eugenia Roupakia because her mentorship and patience played an important role in the completion of this thesis. Her constant encouragement and constructive suggestions have been a tremendous source of motivation. I would also like to thank the other members of the lab, whose encouragement has been pivotal for me.

Lastly, my deepest gratitude goes to my family who have always been there for me. Their unconditional love and constant encouragement have meant the world to me.

Table of Contents

Abstract

Lung cancer continues to be the primary cause of cancer-related mortality globally. This is mainly because it is often diagnosed at advanced stages. Initial symptoms are typically mild or mistaken for common respiratory conditions, which leads to delayed detection and metastatic disease. This limits available treatment options and results in poor prognosis, with fewer than 20% of patients achieving five-year survival.

Extracellular matrix (ECM) stiffness is recognized as a critical regulator of cell behavior, broadly influencing cell signaling pathways that govern growth, survival, and differentiation. The tumor microenvironment in lung cancer can become increasingly stiff and fibrotic. While increased ECM stiffness is associated with cancer progression its role in shaping lung cancer cell behavior and therapy response remains incompletely understood.

In this thesis, polyacrylamide-based hydrogels with tunable stiffness were employed to assess the effects of substrate stiffness on the morphology and proliferation of three EGFR-mutant non-small cell lung cancer (NSCLC) cell lines, namely PC9, HCC4006 and HCC827 cells, as well as their response to the EGFR inhibitor Osimertinib.

We found that on softer matrices PC9, HCC4006, and HCC827 cells exhibit reduced spreading and adopt more circular shapes. Furthermore, all three cell lines demonstrated slower proliferation on soft substrates than on stiffer ones. The impact of matrix stiffness on Osimertinib response was cell line-dependent with HCC827 cells being very sensitive to the drug on both matrices and HCC4006 cells being more sensitive to Osimertinib when they are on softer matrix.

These results underscore the pivotal role of ECM stiffness in modulating lung cancer cell responses to mechanical stimuli and reveal the complex relationship between matrix rigidity and tumor progression. Substrate stiffness significantly influences lung cancer cellular phenotypes, including morphology and proliferation rates, with cells on softer, physiologically relevant substrates exhibiting distinct characteristics compared to those on stiffer substrates. The observed differential responses of EGFR-mutant cell lines to osimertinib treatment indicate that the microenvironment's mechanical properties substantially affect therapeutic outcomes. Further research is necessary to elucidate the mechanisms underlying these effects and to advance the understanding of cancer progression and therapy response.

Περίληψη

Ο καρκίνος του πνεύμονα παραμένει η κύρια αιτία θνησιμότητας που σχετίζεται με τον καρκίνο παγκοσμίως. Αυτό οφείλεται κυρίως στο γεγονός ότι συχνά διαγιγνώσκεται σε προχωρημένα στάδια. Τα αρχικά συμπτώματα είναι συνήθως ήπια ή εκλαμβάνονται ως κοινές αναπνευστικές παθήσεις, γεγονός που οδηγεί σε καθυστερημένη διάγνωση και στην εμφάνιση μεταστατικής νόσου. Ως αποτέλεσμα, οι διαθέσιμες θεραπευτικές επιλογές είναι περιορισμένες και η πρόγνωση παραμένει δυσμενής, με λιγότερο από το 20% των ασθενών να επιτυγχάνουν πενταετή επιβίωση.

Η ακαμψία της εξωκυττάριας θεμέλιας ουσίας (ECM) αναγνωρίζεται ως κρίσιμος ρυθμιστής της κυτταρικής συμπεριφοράς, επηρεάζοντας τις οδούς κυτταρικής σηματοδότησης που ρυθμίζουν την ανάπτυξη, την επιβίωση και τη διαφοροποίηση των κυττάρων. Στον καρκίνο του πνεύμονα, το μικροπεριβάλλον του όγκου μπορεί να γίνει πιο άκαμπτο και ινώδες. Ενώ η αυξημένη ακαμψία της ECM έχει συσχετιστεί με την εξέλιξη του καρκίνου, ο ρόλος της στη συμπεριφοράς των καρκινικών κυττάρων του πνεύμονα και στην απόκρισή τους στη θεραπεία δεν είναι ακόμη απόλυτα κατανοητός.

Στην παρούσα διπλωματική εργασία, υδρογέλες βασισμένες σε πολυακρυλαμίδιο με ρυθμιζόμενη ακαμψία χρησιμοποιήθηκαν για τη διερεύνηση των επιδράσεων της ακαμψίας του υποστρώματος στη μορφολογία και τον πολλαπλασιασμό τριών EGFR-μεταλλαγμένων κυτταρικών σειρών μη μικροκυτταρικού καρκίνου του πνεύμονα, συγκεκριμένα των PC9, HCC4006 και HCC827, καθώς και στην απόκρισή τους στον αναστολέα του EGFR οσιμερτινίμπη.

Διαπιστώθηκε ότι σε μαλακότερα υποστρώματα τα κύτταρα PC9, HCC4006 και HCC827 εμφανίζουν μειωμένη εξάπλωση και υιοθετούν πιο σφαιρικό σχήμα. Επιπλέον, και οι τρεις κυτταρικές σειρές παρουσίασαν βραδύτερο ρυθμό πολλαπλασιασμού σε μαλακά υποστρώματα σε σύγκριση με πιο άκαμπτα. Η επίδραση της ακαμψίας στην απόκριση στην οσιμερτινίμπη αποδείχθηκε εξαρτώμενη από την κυτταρική σειρά, με τα κύτταρα HCC827 να εμφανίζουν υψηλή ευαισθησία στο φάρμακο και στα δύο υποστρώματα, ενώ τα κύτταρα HCC4006 ήταν πιο ευαίσθητα στην οσιμερτινίμπη όταν καλλιεργούνταν σε μαλακότερα υποστρώματα.

Αυτά τα αποτελέσματα υπογραμμίζουν τον κεντρικό ρόλο της ακαμψίας της ECM στη ρύθμιση των αποκρίσεων των καρκινικών κυττάρων του πνεύμονα σε μηχανικά ερεθίσματα και αποκαλύπτουν την πολύπλοκη σχέση μεταξύ της ακαμψίας της θεμέλιας ουσίας και της εξέλιξης του όγκου. Η ακαμψία του υποστρώματος επηρεάζει σημαντικά τη μορφολογία των κυττάρων και τον ρυθμό του πολλαπλασιασμού τους. Οι διαφορετικές αποκρίσεις των κυτταρικών σειρών EGFR στη θεραπεία με οσιμερτινίμπη

υποδηλώνουν ότι οι μηχανικές ιδιότητες του μικροπεριβάλλοντος μπορεί να επηρεάσουν την αποτελεσματικότητα της θεραπείας. Απαιτείται περαιτέρω έρευνα για τη διερεύνηση των υποκείμενων μηχανισμών αυτών των επιδράσεων και για την κατανόηση της εξέλιξης του καρκίνου και της ανταπόκρισης στη θεραπεία.

1. Introduction

1.1. Lung Cancer

1.1.1 Epidemiology of lung cancer

Lung cancer is one of the most common types of cancer globally, accounting for about 13% of all cancer cases and is the leading cause of cancer-related deaths worldwide (***Figure 1***) (Siegel et al., 2024). The disease mainly affects older people, with most diagnoses occurring in individuals aged 65 and older. Despite breakthroughs in diagnostic methods and treatment regiments, lung cancer remains one of the most frequent malignancies (Bradley et al., 2019; Siegel et al., 2020). The persistently high mortality rates are primarily attributed to challenges in early detection and the predominance of advanced-stage diagnoses at the time of clinical presentation (Huang et al., 2025). Early detection of lung cancer remains challenging due to its characteristic lack of specific early symptoms, often leading to diagnoses at advanced stages, significantly hindering prognosis and treatment efficacy (Tang et al., 2025; Wu et al., 2025).

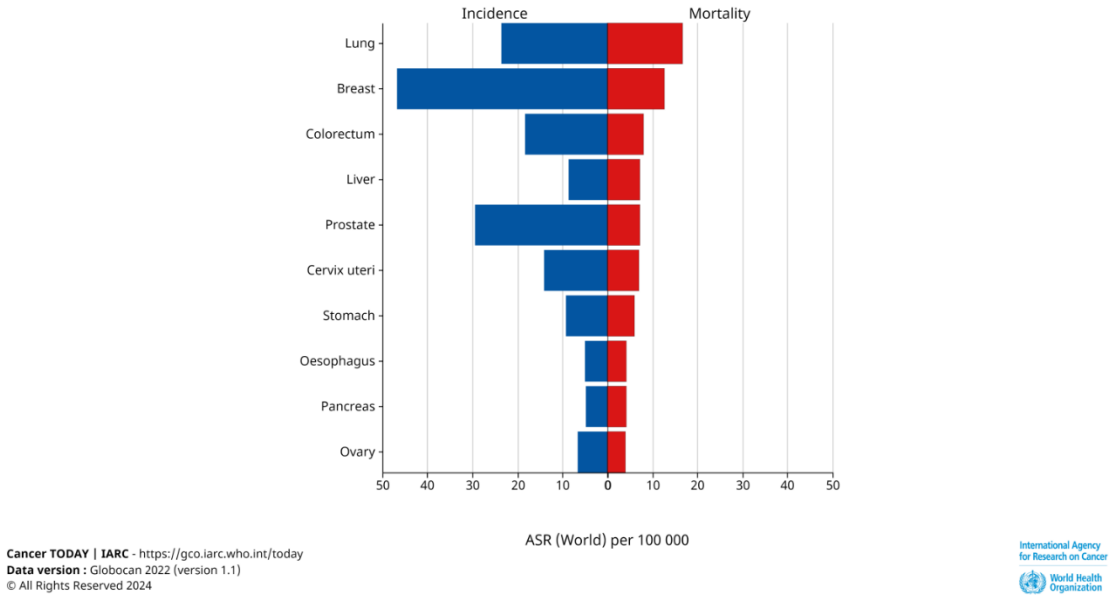

Figure 1. *Estimated age-standardized incidence and mortality rates in 2022, World, both sexes, all ages (Global Cancer Observatory, WHO).*

Lung cancer is categorized into two main types: small cell lung carcinoma (SCLC), which comprises about 15% of all cases, and non-small cell lung carcinoma (NSCLC), which accounts for roughly 85% of the cases (Araghi et al., 2023). Moreover, NSCLC is subclassified into three principal histological subtypes: adenocarcinoma, squamous cell carcinoma, and large cell carcinoma (***Figure 2***). Adenocarcinoma is the most prevalent subtype, accounting for approximately 40% of all lung cancer cases, and it is associated with a low 5-year survival rate of approximately 15%, due to late-stage diagnosis and drug resistance, in comparison to squamous cell carcinoma and large cell carcinoma which are less prevalent (Chen et al., 2014; Zappa & Mousa, 2016). The standard approach for identifying these NSCLC subtypes relies primarily on immunohistochemical assays, followed by molecular analysis of the tumor. In the past two decades, the integration of molecular techniques into pathological diagnosis has enabled more precise categorization of lung cancers. This has greatly improved diagnostic accuracy, going beyond traditional histopathology to include genetic and molecular changes (Pisano et al., 2022).

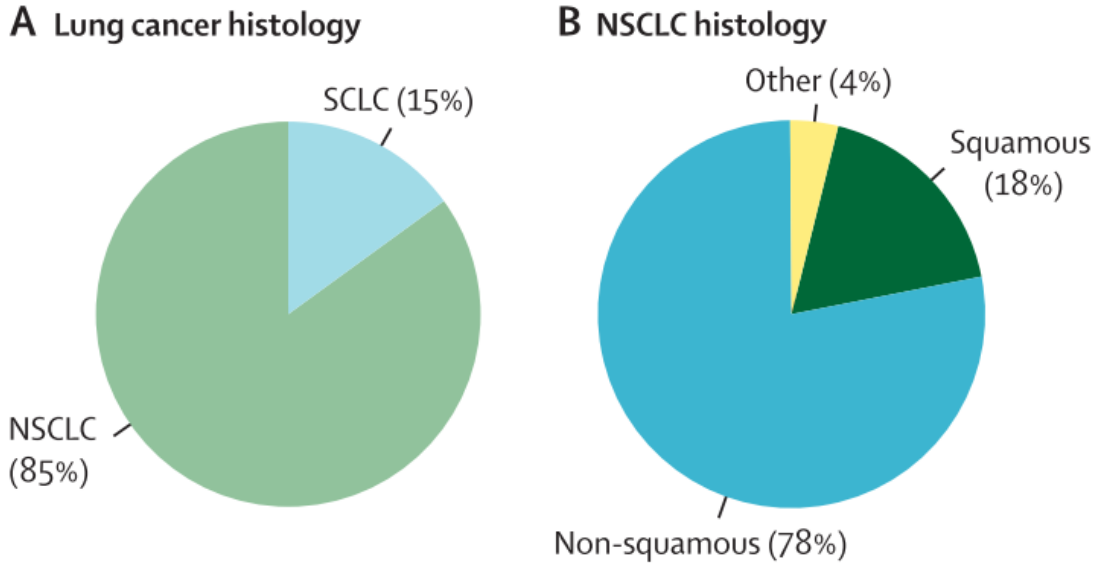

Figure 2. *Lung Cancer histology. Lung cancers are classified into SCLC or NSCLC (A), with the latter further subdivided into squamous and non-squamous (B). Adapted from (Thai et al., 2021).*

1.1.2 Histology of NSCLC

Adenocarcinoma typically arises from type II alveolar epithelial cells that secrete mucus. It develops in the peripheral regions of the lung and is observed in both smokers and non-smokers from both genders. Its peripheral location is thought to be associated with cigarette smoke filtration, which allows deeper inhalation, leading to the development of tumors in the outer lung areas. Adenocarcinoma tends to grow more slowly than other NSCLC subtypes, often resulting in earlier detection and potentially better outcomes compared to central tumors (Zappa & Mousa, 2016). Conversely, squamous-cell carcinoma arises centrally from the bronchial epithelium and is strongly associated with cigarette smoking. Large cell carcinoma, representing 5–10% of lung cancers cases, is characterized by poorly differentiated cells and often presents with early invasion of lymph nodes and distant organs (Zhang et al., 2023).

1.1.3 Epidemiology and Molecular Heterogeneity

Molecular profiling has revealed significant heterogeneity within NSCLC, with key driver mutations influencing therapeutic decisions. Common genetic alterations include mutations in KRAS and EGFR genes and ALK, and ROS1 rearrangements (***Figure 3***).

Mutations of the EGF receptor is the second most frequent alteration, detected in 15–20% of NSCLC cases, with higher prevalence among non-smokers, females, and Asian populations (Melosky et al., 2022) More often *EGFR* mutations occur within the tyrosine kinase domain and consist mainly of exon 19 deletions (54%) and the L858R point mutation in exon 21 (41%) (Riely et al., 2024). These alterations lead to constitutive activation of the receptor, promoting cellular proliferation and survival. The diverse landscape of oncogenic drivers also includes BRAF, MET, and HER2 alterations, alongside NTRK and RET fusions (***Figure 3***), underscoring the necessity for comprehensive genomic profiling to guide targeted therapeutic strategies (Friedlaender et al., 2024).

Kras is a small GTPase that functions downstream of receptor tyrosine kinases such as EGFR and becomes activated upon ligand stimulation. In NSCLC, oncogenic KRAS mutations impair its intrinsic GTPase activity and therefore lock the protein in its active, GTP bound state. Constitutively active KRAS drives continuous activation of downstream effectors, especially the RAF–MEK–ERK and PI3K–AKT pathways. As a result, it drives ongoing transcriptional programs that support cell cycle progression, survival, and metabolic changes, independently of ligand (Nussinov et al., 2016; Zhong et al, 2016).

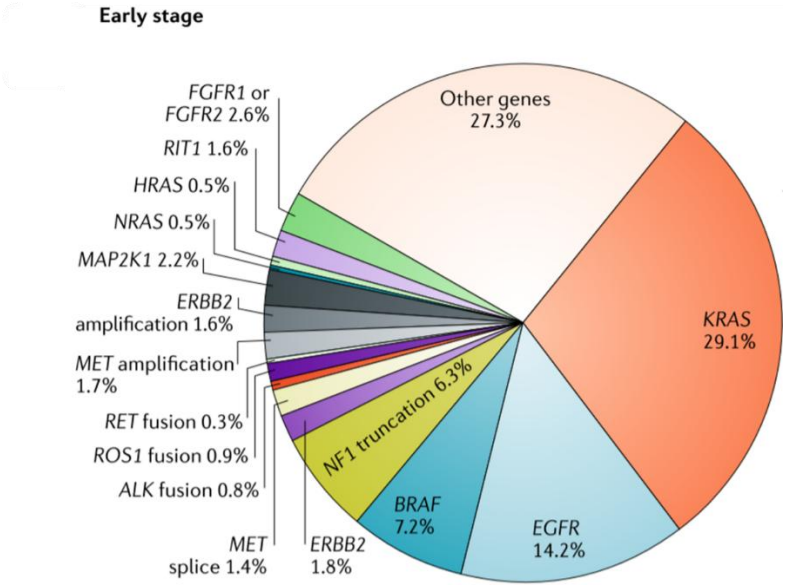

***Figure 3**. Pie chart of oncogenic driver mutations in early-stage lung adenocarcinoma. Adapted from* (Skoulidis & Heymach, 2019).

ALK, ROS1, RET, and NTRK fusions produce chimeric receptor tyrosine kinases. The partner gene provides dimerization domains, which lead to constant, ligand-independent activation of the kinase domain and sustained downstream signaling (Di Marco & Voena, 2022; Mulkidjan et al., 2023). Oncogenic BRAF mutations, usually activating mutations or fusions in the kinase domain, also cause ongoing MEK–ERK pathway signaling, bypassing upstream control and leading to unchecked cell-cycle progression (Yan et al., 2022).

MET alterations in lung cancer, such as exon 14 mutations, stabilize the MET receptor and increase its kinase activity. This maintains activation of the downstream PI3K–AKT and RAS–MAPK signaling and often serve as an alternative signaling pathway when other oncogenic pathways are inhibited (Zhang et al., 2019). HER2 (ERBB2) alterations, including exon 20 insertions, promote constitutive HER2 homo- or heterodimerization and ongoing activation of PI3K–AKT and RAS–RAF–MEK–ERK signaling. This supports cell growth, survival, and epithelial–mesenchymal transition in NSCLC cells (Ismail et al., 2025; Peters & Zimmermann, 2014).

1.2 Extracellular Matrix (ECM)

The ECM is a three-dimensional, non-cellular network essential for maintaining tissue organization and function in organisms (Jiang et al., 2022). Its primary components are collagens and proteoglycans (Zbek et al., 2010). Composed of approximately 300 distinct molecules, the ECM provides structura and biochemical support to cells, tissues, and organs. Glycosaminoglycans and proteoglycans interact with growth factors and matrix proteins to regulate cell proliferation (Yue et al., 2014). Glycosaminoglycans also bind water, acting as lubricants and shock absorbers, facilitating cell migration, and organizing collagen deposition. These features enable the ECM to withstand high compressive forces (Farach-Carson et al., 2024).

The dynamic ECM consists of two main components: basement membranes and the interstitial matrix (***Figure 4***) (Hynes et al., 2009). Basement membranes provide structural support, regulate cell polarity, and bind growth factors and cytokines that control differentiation and maintain tissue homeostasis (Hynes et al., 2009).

In contrast, the interstitial matrix forms a permeable three-dimensional scaffold that surrounds cells, connecting them to each other and to the basement membrane (Egeblad et al., 2010). It is rich in fibrillar collagens, proteoglycans, and glycoproteins such as tenascin C and fibronectin, making it highly charged and hydrated, which contributes to tissue tensile strength (Egeblad et al., 2010). When organized, ECM components provide unique physical and biomechanical properties essential for regulating cell behavior. The matrix can also initiate signaling events by serving as a precursor for biologically active fragments (Hynes et al., 2009)

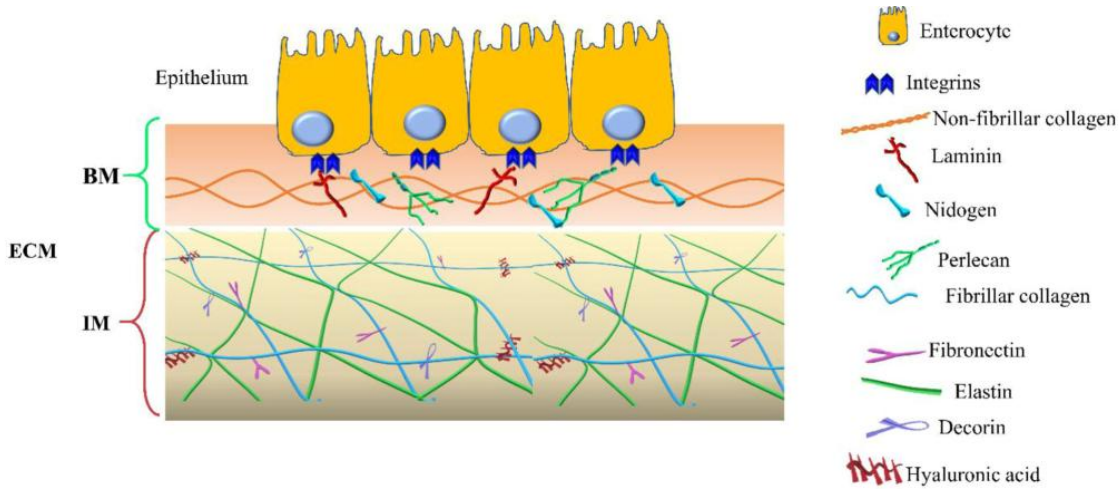

Figure 4*. ECM compartments. Schematic representation of the main components of the two ECM compartments: basement membrane (BM) and interstitial matrix (IM). The legend indicates the identity of each ECM component. Adapted from (Pompili et al., 2021).*

ECM undergoes significant alterations in response to disease or trauma, which can severely compromise tissue integrity and function. For instance, fibrotic or scar tissue that forms following injury displays structural properties that differ substantially from those of healthy tissue. Excessive ECM deposition is a defining feature of fibrosis (Keane et al., 2018).

In cancer, tumors manipulate ECM remodeling to establish a microenvironment that supports tumorigenesis and metastasis. These tumor-induced changes promote tumor growth, increase tumor cell migration, and prepare distant organs for metastasis through ECM modification. Comprehensive understanding of these ECM remodeling mechanisms is crucial for the development of effective therapies (Joyce & Pollard, 2009).

Continuous interactions between the ECM, tumor cells, immune cells, and cancer-associated fibroblasts profoundly influence tumor progression, metastasis, immune modulation, and metabolic reprogramming. These processes highlight the central role of the ECM in cancer biology. The biophysical properties of the ECM, such as stiffness, viscoelasticity, and permeability, are increasingly recognized as key regulators of tumor behavior, with stiffness identified as particularly important (Zhang & Zhang, 2025).

1.2.2 Matrix stiffness in health and cancer

ECM stiffness, also known as the modulus of elasticity, is a fundamental biomechanical property that describes its resistance to deformation under mechanical stress. It is quantitatively measured in kilopascals (kPa), where 1 Pa equals 1 N/m² (one Newton of force per square meter) (Feng et al., 2024). In healthy tissues, the ECM undergoes continuous degradation and remodeling to preserve tissue integrity and function, including the synthesis of new matrix proteins to replace degraded components (Lu et al., 2011). This dynamic equilibrium is regulated by the interplay between matrix metalloproteinases and their inhibitors, particularly tissue inhibitors of metalloproteinases, as well as enzymes such as lysyl oxidase. In most solid tumors, this regulatory balance is disrupted due to the activation of cancer-associated fibroblasts (Lu et al., 2011; Pan et al., 2025). These cells promote fibrotic stromal hyperplasia and increased ECM cross-linking, which collectively result in elevated matrix stiffness (Wei et al., 2022).

In cancer, the ECM undergoes substantial modifications that facilitate tumor growth and metastasis (***Figure 5***) (Petrik et al., 2010). These alterations encompass changes in the composition, structure, and regulation of the ECM (Dzobo & Dandara, 2023). Key elements of the tumor microenvironment, including cancer-associated fibroblasts,

contribute to both ECM stiffening and degradation, thereby promoting tumor progression (Najafi et al., 2019). Additionally, reciprocal interactions occur between cancer cells and the ECM, wherein cancer cells remodel the ECM, and in turn, the ECM modulates cancer cell behavior (Endo & Inoue, 2019; Popova & Jücker, 2022)

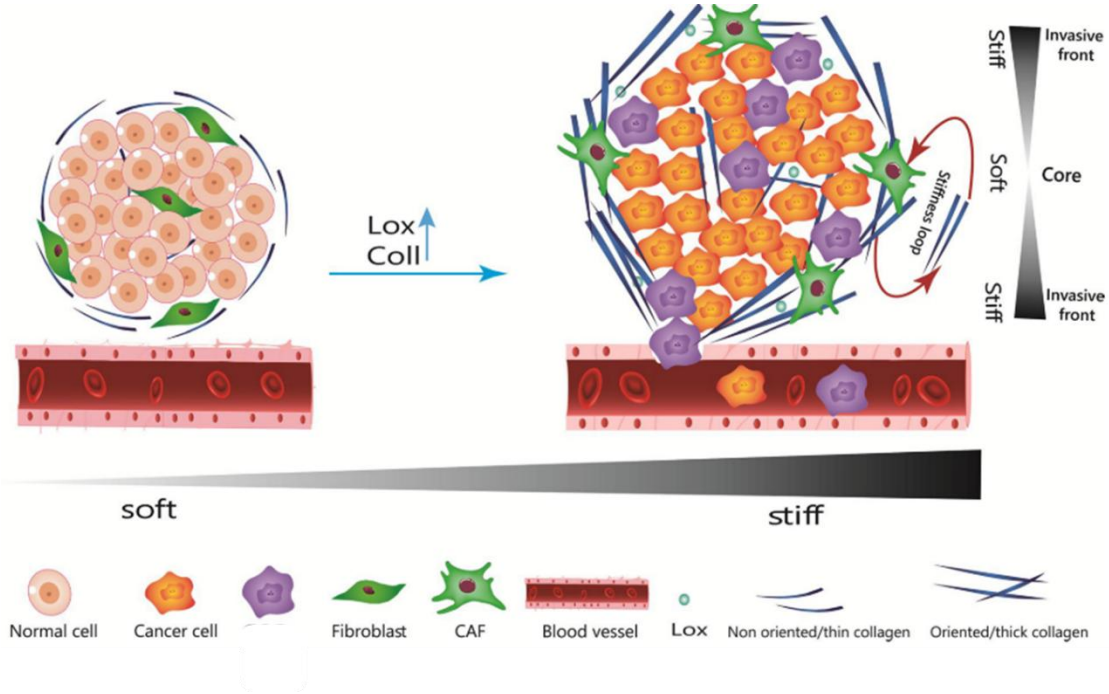

Figure 5. *Alterations in tumor matrix stiffness: normal organs are surrounded by collagen, which forms an ECM that is compliant and soft. In several solid tumors, the accumulation of ECM proteins causes a gradual rise in matrix stiffness parallel with the tumor's growth. Tumor cells and other TME cells, particularly CAFs, produce collagen and Lysyl oxidase (LOX), resulting in collagen crosslinking, ECM rearrangement, and increased stiffness. In addition, increasing stiffness within tumors contributes to the continuous activation of CAFs, establishing a feed-forward loop that aids in the formation of a permanently stiff tumor niche. The invasive tumor front is stiffer than the tumor's core. Adapted from (Safaei et al., 2023).*

Under physiological conditions, each organ in the human body exhibits a characteristic stiffness (***Figure 6***) (Wells et al., 2013). Pathological conditions, such as fibrosis and cancer, disrupt this homeostasis and result in altered organ stiffness. In cancer, tumor tissues typically display increased stiffness relative to healthy tissues, with values ranging from 1 kPa in brain tumors to 70 kPa in cholangiocarcinoma (Jain et al., 2014).

The stiffness of lung cancers is approximately 20–30 kPa, substantially greater than the 0.2kPa observed in normal lung parenchyma (Ishihara & Haga, 2022; Park et al., 2024). Similarly, pancreatic cancer tissues can exceed 6 kPa, a notable increase from the 1–3 kPa of healthy pancreatic tissue, indicating disease states like fibrosis or cirrhosis (Huang et al., 2025; Ishihara & Haga, 2022; Kpeglo et al., 2022). Additionally,

in breast, tissue stiffness was measured to be several times stiffer than normal breast tissue (Ishihara & Haga, 2022; Kraning-Rush & Reinhart-King, 2012). This elevated stiffness has emerged as a critical determinant in regulating tumor progression and metastasis, serving as a diagnostic and prognostic marker.

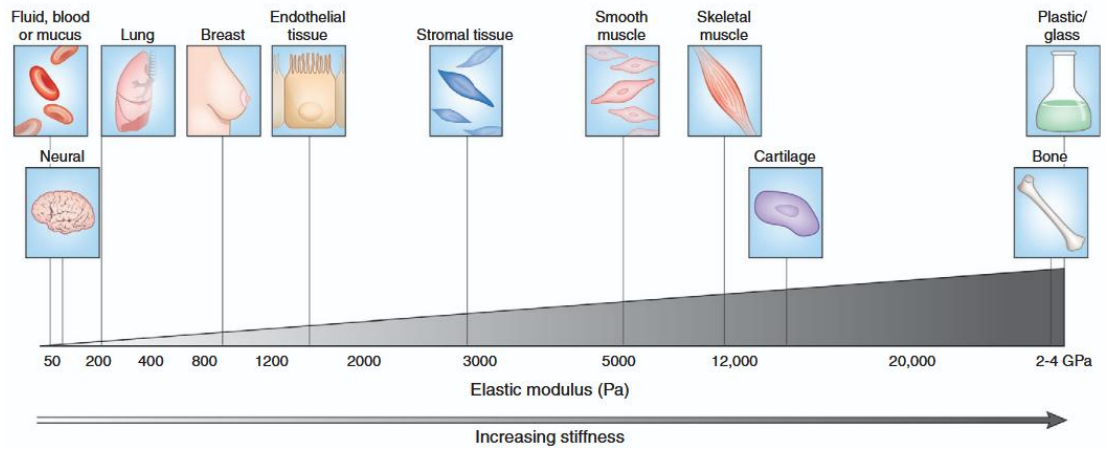

Figure 6. *Variations in tissue stiffness. Mechanically static tissues such as brain or compliant tissues such as lung exhibit low stiffness, whereas tissues exposed to high mechanical loading, such as bone or skeletal muscle, exhibit elastic moduli with a stiffness that is several orders of magnitude greater. Adapted from* ***(Cox & Erler, 2011)****.*

The response of epithelial cells to matrix stiffness is mediated by an intricate mechanotransduction cascade, in which cells sense mechanical signals in their environment and activate intracellular signaling pathways. These pathways involve integrin clustering and activation of focal adhesion kinase (FAK), the Rho/Rho-associated protein kinase (ROCK) pathway, and the extracellular signal-regulated kinase (ERK) pathway (Desai et al., 2016). Integrins serve as primary mechanotransduction sensors within cells (Ross et al., 2013).

1.2.3 ECM in pulmonary cancer

The lung's ECM comprises various core matrisomal proteins that provide structural support, along with enzymes that remodel these proteins and soluble factors linked to the matrix. These proteins work together as a dynamic network that is constantly being remodeled. Compared with normal lung tissue, primary lung tumors display significant changes in these matrisomal proteins (Zhou et al., 2018). Differences in the composition and structure of the ECM in the central airways and distal parenchyma strongly influence how these lung region's function (Burgess et al., 2016; Zhou et al., 2018). Studies have linked ECM composition in NSCLC tumors to the risk of disease recurrence (***Figure 7***), suggesting that the ECM regulates cancer spread, dormancy, or growth in the lungs and other sites (Parker & Cox, 2020).

Within the central lung, the ECM is primarily composed of fibrillar collagens, particularly types I and II. Conversely, the alveoli in the distal lung contain a more loosely organized network, predominantly consisting of type I and II collagens and elastin (Hoffman et al., 2023; Zhou et al., 2018). Resident fibroblasts, aided by lysyl oxidase family enzymes, maintain this ECM composition to preserve tissue homeostasis (DeLeon-Pennell et al., 2020; Zaffryar-Eilot & Hasson, 2022). Alterations in collagen content during lung cancer development or fibrosis underscore the critical role of these protein fibers in maintaining lung structure and function (Onursal et al., 2021).

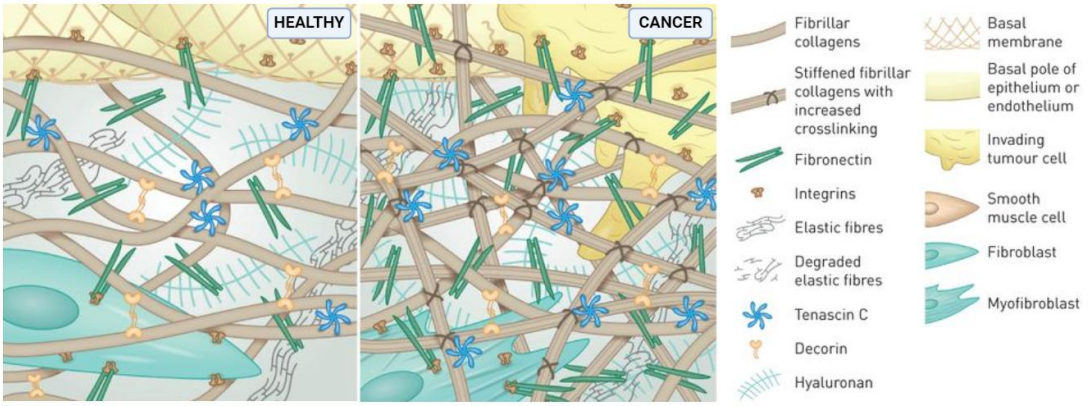

Figure 7. *Differences between healthy and malignant pulmonary ECM. Adapted from (Burgstaller et al., 2017).*

1.3. Epidermal Growth Factor Receptor (EGFR)

Epidermal Growth Factor Receptor (EGFR), also known as ErbB1 or HER1, is a transmembrane glycoprotein that functions as a receptor tyrosine kinase (RTK). Discovered initially in the 1960s EGFR plays a fundamental role in regulating cellular growth, proliferation, differentiation, and survival (Zeng & Harris, 2014). It belongs to the larger ErbB family, which includes ErbB2, ErbB3, and ErbB4, all of which are transmembrane proteins with intrinsic tyrosine kinase activity (Berasain & Avila, 2014). In normal cells, EGFR activation is tightly regulated, but in cancer cells it becomes dysregulated through activating mutations, overexpression, or increased ligand production (Uribe et al., 2021). Dysregulation of EGFR, through gene mutations or amplification, has been definitively linked to cancer initiation, progression, and poor prognosis across various malignancies, including non-small cell lung cancer, colorectal cancer, and squamous cell carcinoma of the head and neck (Yamaoka et al., 2017).

1.3.1 The EGFR Kinase Domain: Structure and the Molecular Pathways Driving Malignant Transformation.

Structurally, EGFR is composed of an extracellular ligand-binding domain, a single transmembrane helix, an intracellular portion that contains the tyrosine kinase domain and a C-terminal phosphorylation region (***Figure 8***) (Ferguson et al., 2008; Lee et al., 2006). Upon the binding of ligands, such as EGF or transforming growth factor-alpha, the receptor undergoes dynamic conformational changes and forms homo- or heterodimers (***Figure 8***). This dimerization event stimulates the receptor's intrinsic tyrosine kinase activity (Dawson et al., 2005; Purba et al., 2017).

Subsequently, this activation leads to the trans-autophosphorylation of specific tyrosine residues located within both the kinase domain and the C-terminal tail (Yamaoka et al., 2017). These phosphorylated tyrosine residues then serve as critical docking sites for a variety of intracellular signaling molecules. These include kinases, adaptor proteins, ubiquitin ligases, and transcriptional factors, which contain Src homology 2 domains (Wagner et al., 2013; Yamaoka et al., 2017). The recruitment and binding of these signaling molecules to the activated EGFR ultimately initiate and activate several downstream signaling pathways, such as the RAS/RAF/MAPK/ERK pathway and the PI3K/AKT/mTOR pathway (Wee & Wang, 2017).

These pathways are fundamental for regulating various cellular processes, including cell proliferation and survival (Asati et al., 2016; Mendoza et al., 2011; Yamaoka et al., 2017). Overexpression of wild-type EGFR or kinase-activating mutations can further enhance cell proliferation, migration, survival, and antiapoptotic responses through these signaling cascades (Ayuso-Sacido et al., 2010; Wee & Wang, 2017). The disruption of proper EGFR signaling due to overexpression or activating mutations within EGFR promotes tumor growth (Gazdar & Minna, 2008). Constitutive activation of EGFR by gene mutations or amplification is related to cancer initiation, progression, and poor prognosis in several cancers, including non-small cell lung cancer (Yamaoka et al., 2017).

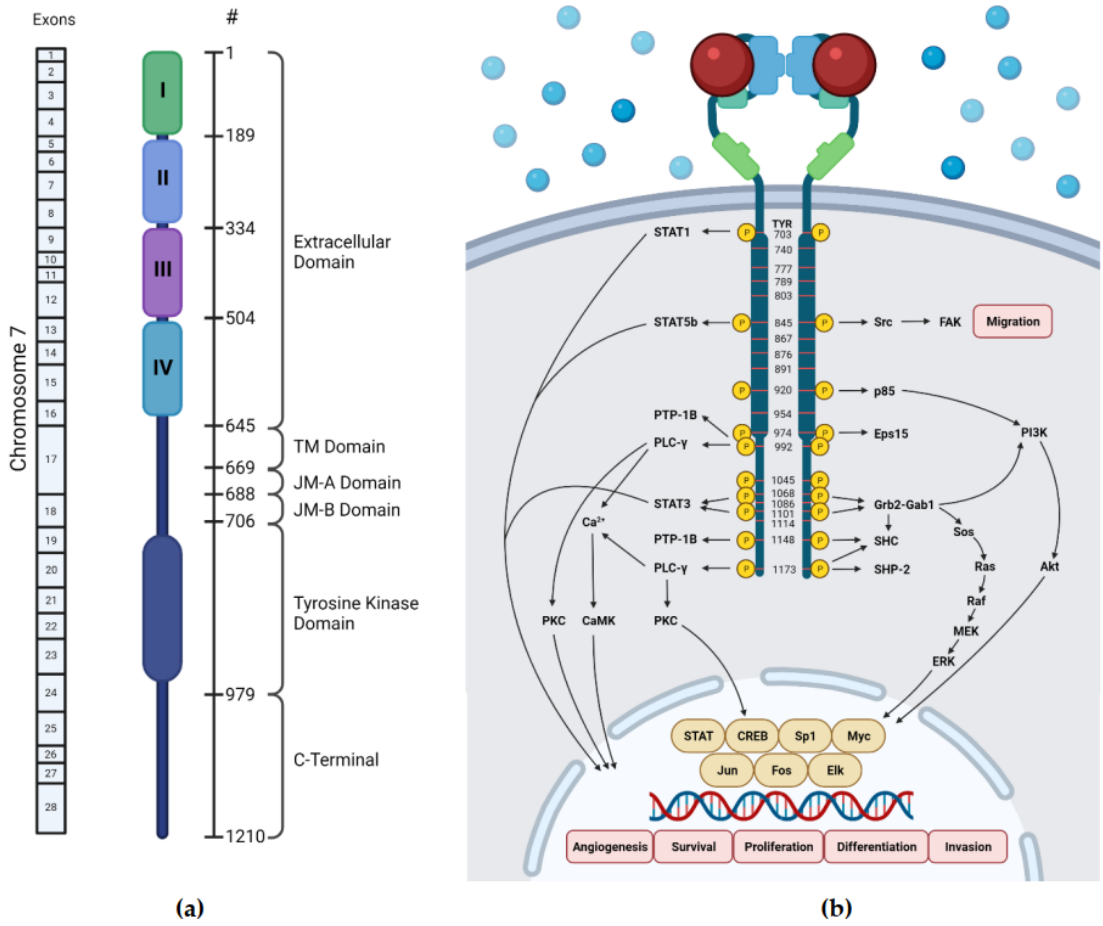

***Figure 8**. Schematic diagrams of EGFR domains and downstream pathways (a) Domain structure of human EGFR and exons encoding it, (b) EGFR phosphorylation sites and downstream pathways. Blue spheres indicate the molecules present outside the cell, and red spheres indicate the EGFR activating ligand. Adopted from (Amelia et al., 2022).*

Most oncogenic mutations associated with lung cancer occur within the kinase domain of the epidermal growth factor receptor. The predominant mutations are in-frame deletions in exon 19 and the L858R point mutation in exon 21 (***Figure 9***). These "classic" activating mutations collectively account for approximately 85-90% of all EGFR mutations found in non-small cell lung cancer (Li et al., 2008; Zhang et al., 2010).

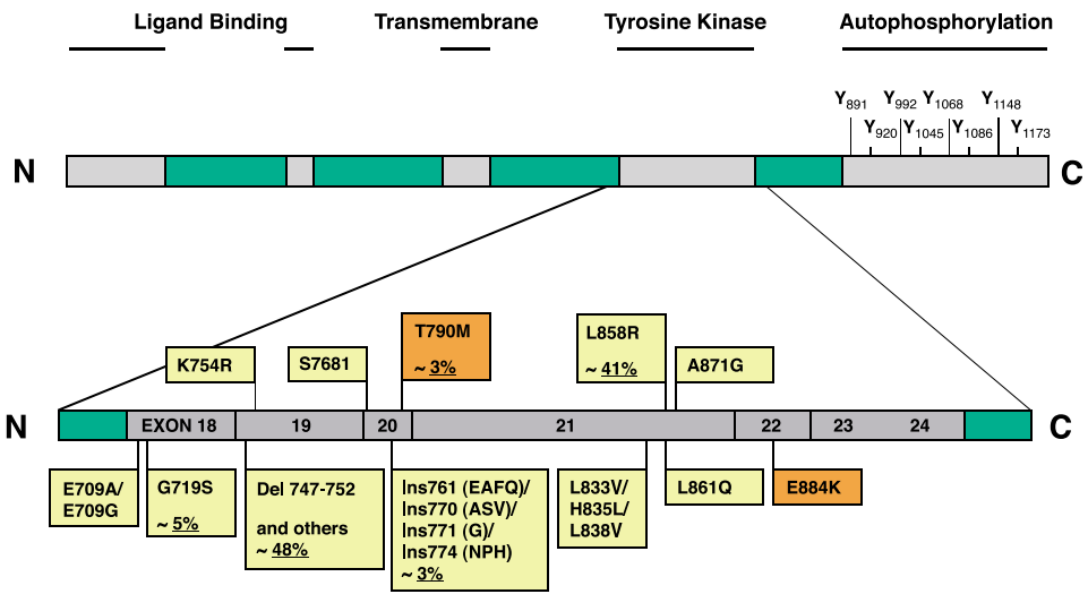

***Figure 9**. EGFR kinase domain mutations in NSCLC. Structural organization of EGFR and localization of clinically relevant alterations in the kinase domain (yellow boxes). Frequencies are indicated and mutations that may confer resistance to gefitinib (T790M) or erlotinib (T790M, E884K) are highlighted (orange boxes). Adapted from (Irmer et al., 2007).*

Exon 19 deletions typically involve a small in-frame removal of amino acids, often encompassing codons L747 to E749 (***Figure 9***) (Su et al., 2017). These deletions cause a conformational change in the EGFR, leading to its constitutive activation, meaning the receptor is active without requiring ligand binding (Guo et al., 2015). The L858R mutation is a substitution of leucine with arginine at codon 858 in exon 21 (Sutto & Gervasio, 2013). This mutation is located within the activation loop of the kinase and stabilizes the EGFR kinase domain in its constitutively active conformation (Yun et al., 2007). Both types of mutations activate EGFR, leading to increased cell proliferation and anti-apoptotic signaling pathways. These activating mutations are critical because they result in ligand-independent activation of growth pathways, driving malignant transformation in NSCLC. Patients whose tumors harbor these specific EGFR mutations often show sensitivity to EGFR tyrosine kinase inhibitors (Guo et al., 2015; Sutto & Gervasio, 2013).

1.3.2 Epidermal Growth Factor Receptor inhibitors (EGFR-TKIs)

First-generation EGFR inhibitors, such as erlotinib and gefitinib, have demonstrated significant clinical benefit in patients with tumors harboring activating EGFR mutations (He et al., 2021). However, the duration of response to these agents is limited, primarily due to the emergence of secondary resistance mutations. One of the most common resistance mechanisms involves the acquisition of a T790M mutation, which occurs in approximately 60% of cases after initial therapy (Costa et al., 2008; He et al., 2021). This “gatekeeper” mutation alters the ATP-binding pocket of EGFR, increasing its affinity for ATP and diminishing the binding efficacy of first-generation TKIs (Cross et al., 2014; Sequist et al., 2011).

To overcome this resistance, third-generation EGFR inhibitors such as osimertinib were developed (Mccoach et al., 2016). Osimertinib is a potent, irreversible inhibitor that has significantly improved treatment outcomes for non-small cell lung cancer patients harboring specific EGFR mutations (Ricciuti & Chiari, 2018; Zhang et al., 2020). It covalently binds to the cysteine residue at position 797 within the kinase domain, targeting both EGFR-sensitizing mutations and T790M-mediated resistance mutations (***Figure 10***) (Leonetti et al., 2019). Clinical trials have also established that osimertinib offers substantial benefits in both first line and subsequent treatment settings, leading to its widespread adoption as a standard therapy for EGFR-mutant non-small cell lung cancer (Criscione et al., 2022).

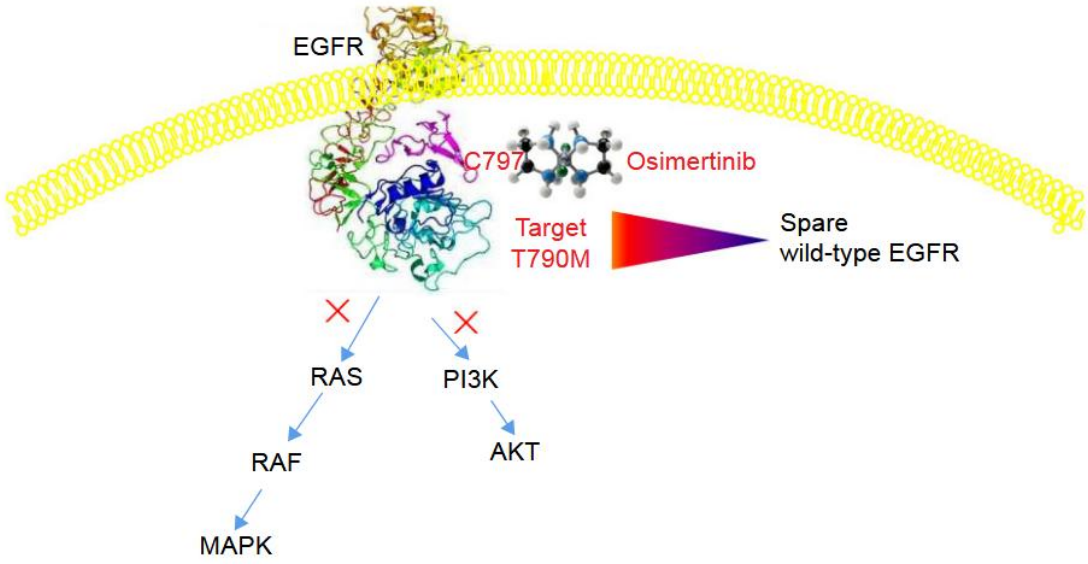

Figure 10. Schematic illustration of the possible mechanism of action of osimertinib. Adapted from (Zhang et al., 2016).

Despite its efficacy, resistance to osimertinib frequently develops, with the C797S mutation emerging as principal mechanism of acquired resistance (Chmielecki et al., 2023; Liao et al., 2025). This mutation affects the covalent binding site of osimertinib, reducing its ability to inhibit EGFR and ultimately leading to disease progression (Li et al., 2023). Additionally, recent research indicates that the tumor microenvironment plays a critical role in mediating treatment response and resistance. However, a considerable proportion of patients who experience disease progression on osimertinib do not present with any known resistance mutations, thereby complicating treatment strategies (Liao et al., 2025; Piotrowska et al., 2018).

In particular, a subset of cancer cells can survive initial osimertinib exposure by entering a reversible, drug-tolerant persister (DTP) state (Cabanos & Hata, 2021). These DTPs are not inherently resistant but serve as a reservoir from which durable resistance mechanisms can develop over time, ultimately contributing to disease relapses (Dhanyamraju et al., 2022; Liu et al., 2025). The survival and adaptation of these cells are influenced by various factors within the tumor microenvironment, and understanding their biology is crucial for developing strategies to improve long-term treatment efficacy (Izumi et al., 2024).

1.4 In vitro polyacrylamide hydrogels for cancer studies

Hydrogels are crosslinked polymeric networks that can uptake and retain large amounts of aqueous fluids (Ho et al., 2022). They are considered to be valuable tools for modeling extracellular environments and probing cellular behavior in vitro due to their ability to mimic the ECM that supports living cells in their native microenvironment (Vieira et al., 2022). These models offer direct control over ECM aspects, enabling investigation into the effects of various extracellular properties on cell behavior. The ability to tune key properties of the extracellular environment, such as stiffness (Pérez-Calixto et al., 2021; Subramani et al., 2020), viscoelasticity (Cacopardo et al., 2019) cell adhesion motifs, and presentation of biochemical cues (Vieira et al., 2022) has been demonstrated by various groups. Therefore, hydrogels with regulated properties are extensively used as supporting materials in cell biology, tissue engineering and regenerative medicine applications (Wolfel et al., 2022).

In this context, polyacrylamide (PA) hydrogels have been among the most popular materials for 2D cell culture and cell mechanical studies in general. PA hydrogels present important advantages that explain their extended use in cell biology laboratories in the last 25 years. They are ideal for these studies because they are mechanically tunable and their stiffness, measured as Young's modulus (E), can be

precisely tuned from tens of pascals to hundreds of kilopascals by simply changing the concentrations of the monomer (acrylamide) and crosslinker, (bis-acrylamide) (Pérez-Calixto et al., 2021; Pineda-Hernandez et al., 2025). Typically, their polymerization process occurs via acrylic-based free radical polymerization (FRP) of acrylamide (AA) and the crosslinker bis-acrylamide (bis-AA), using persulfate and TEMED as redox initiators (***Figure 11***).

Another advantage is that they are optically transparent, and their thin, translucent quality makes them compatible with microscopy at high magnifications (Tse & Engler, 2010). They are also low-cost and their synthesis require chemically simple compounds thus they can be easily synthesized in almost any lab (Vignaud et al., 2014). The pore sizes of the gels are on the order of 100 nm, preventing cells and their extensions from entering the substrate. (Flanagan et al., 2002.).

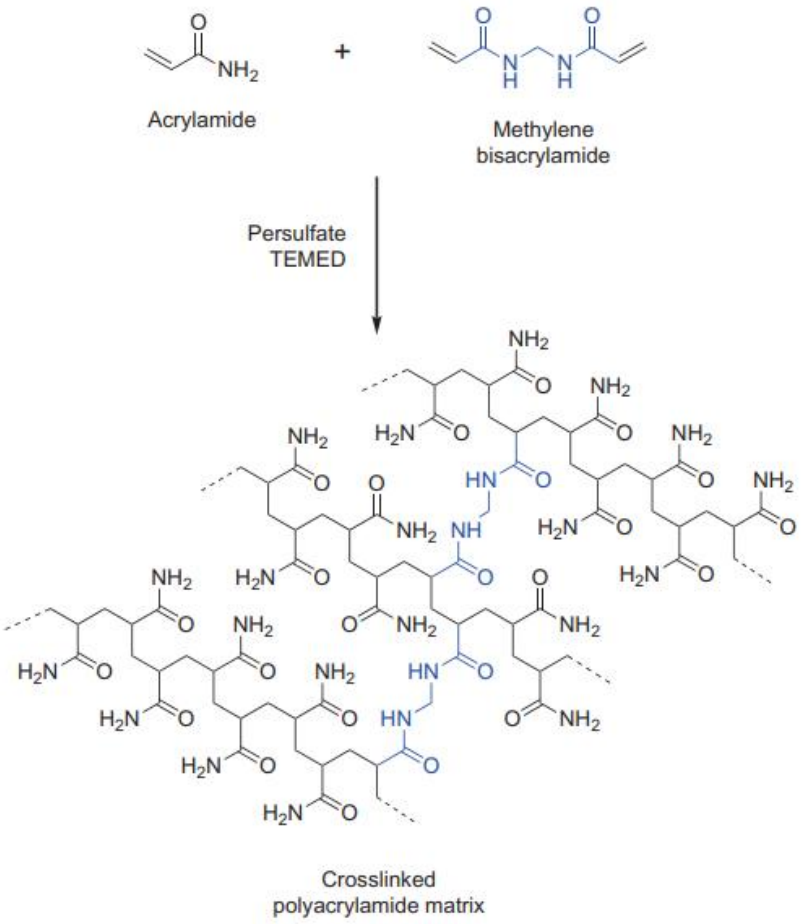

Figure 11*. Polyacrylamide supports are made from the copolymerization of acrylamide and the crosslinking monomer N,N'-methylene bisacrylamide. The ratio of crosslinking monomer to acrylamide monomer controls the degree of porosity in the final support material. Adapted from (Hermanson et al., 2013).*

Another characteristic of PA hydrogels is that they are chemically stable and have strong protein-repellent properties, which means they resist cell adhesion. Therefore, careful biofunctionalization is essential to add bioactivity and promote strong interactions between cells and materials (Wolfel et al., 2022) Importantly, these modifications need to occur under gentle conditions to protect the structure and function of attached ligands. To achieve this, new chemical methods have been developed for precise bonding of ligands to PA gels. One popular method uses Sulfo-SANPAH, a versatile crosslinker activated by UV light, as shown in ***Figure 12***. UV light changes the nitrophenyl azide into a highly reactive nitrene, creating strong covalent bonds with polyacrylamide's carbon-hydrogen framework. At the same time, the sulfosuccinimidyl part of Sulfo-SANPAH strongly bonds with primary amines of ECM proteins used for hydrogel coating. The process allows for coating the hydrogels with a type I collagen solution, turning the passive surface into a dynamic, cell-adhesive area that mimics the ECM in 2D cell culture scaffolds (Tse & Engler, 2010).

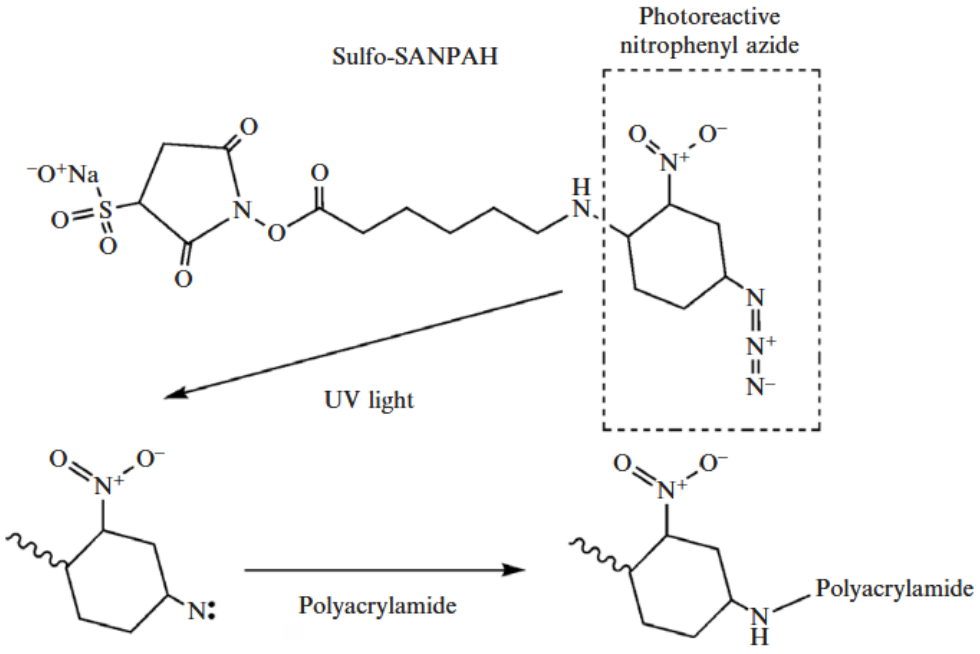

Figure 12. *The heterobifunctional photoreactive reagent sulfo-SANPAH. When the nitrophenyl azide reactive group is exposed to UV light (320–350 nm), it forms a nitrene group that can react nonspecifically with polyacrylamide. The sulfosuccinimydyl group at the other end reacts with primary amine groups of the protein. Adapted from (Kandow et al., 2007).*

Once the cells are seeded on these biofunctionalized hydrogels, they form crucial connections and apply significant forces on their environment. The composition of the

matrix and its mechanical properties greatly influence cell shape and spreading. Polyacrylamide hydrogels can be precisely adjusted through crosslinking density to effectively mimic various microenvironments that influence how far cells can extend. "Stiffer" gels, which have higher bis-acrylamide-to-acrylamide ratios, resist changes in shape, encouraging cells to spread out or elongate. On the other hand, "softer" gels with lower ratios bend easily, forcing cells into small, rounded shapes that lack the ability to stretch. This level of control over stiffness allows for groundbreaking studies on how mechanical cues in the environment affect cell growth, adhesion, movement, and spreading (Crandell & Stowers, 2023; Worthen et al., 2017).

2. Motivation and Aims

The overall goal of this research project was to elucidate the impact of matrix stiffness on lung cancer cell behavior and their response to drug treatment *in vitro*. More specific objectives were

1. Fabrication and validation of PA hydrogels with tunable stiffness
2. To study how lung cancer cells alter their morphology in response to various matrix stiffnesses
3. To elucidate the impact of matrix stiffness on the growth of lung cancer cells
4. To evaluate the influence of matrix stiffness on the response of lung cancer cells to EGFR inhibition

To achieve this, we cultured EGFR-driven NSCLC cell lines (PC9, HCC827 and HCC4006 cells) on hydrogels with varying substrate stiffnesses (0.1–100 kPa) as well as on glass to replicate the physiological environments of both normal and cancerous lung tissues. These experiments provided insights into the effects of stiffness on cancer cell morphology and proliferation. Furthermore, to investigate how matrix stiffness influences cancer cell responses to treatment, we administered the third-generation EGFR-TKI osimertinib to the cell cultures at varying concentrations and assessed cell viability.

3. Materials and Methods

3.1 Cell Culture

3.1.1 Cell Culture and Sub-culturing

Three lung adenocarcinoma cell lines that harbor EGFR mutations were cultured in RPMI complete medium (Sigma, cat. No. R8758-500ML), supplemented with 10% Fetal Bovine Serum (FBS) (Biowest, cat. No. S181B-500), 1% Penicillin-Streptomycin (Biowest, cat. No. L0022-100), and 1% L-Glutamine (Biowest, cat. No. X0550-100). Cells were tested for mycoplasma contamination and incubated at +37°C in a humidified incubator with 5% CO_2. The specifics for each cell line and their oncogenic mutations are listed in ***Table 1***.

Table 1. *Cell lines used in the following experiments*

Cell line(s)	EGFR	NSCLC subtype	Primary/metastasis
HCC-827	E746_A750del	Adenocarcinoma	Primary
HCC-4006	L747_E749del	Adenocarcinoma	Metastasis (from pleural effusion)
PC9	E746_A750del	Adenocarcinoma	Primary

The cells were subcultured every 3 days or when cells reached 80-90% confluency. The cells were washed once with 1x Phospate Buffered Saline (PBS) prior to being detached with 1xTrypsin-EDTA. The detached cells were suspended into the complete culture medium to inactivate the trypsin.

The number of cells used for each cell line varied depending on the nature of each experiment. To assess cell morphology, 2500 cells/well (PC9, HCC827, and HCC4006) were seeded on 96-well plates coated with hydrogels of varying stiffness (Matrigel, HTP plates). For proliferation experiments, 25000 cells/well (PC9, HCC827 and HCC4006) were seeded on in-house fabricated soft and stiff hydrogels. Their proliferation was assessed by monitoring daily cell confluency in IncuCyte zoom. At last, the impact of stiffness on drug treatment was examined using our homemade stiff and soft hydrogels (HCC827 and HCC4006) and hydrogels of varying stiffness for PC9 cell line (Matrigel, HTP plates). For HCC827, 75000 cells/well were plated on stiff and soft hydrogels, for HCC4006, 50000 cells/well were plated on soft hydrogels, and 40000 cells/well were plated on stiff hydrogels and for PC9 1500 cells/well were plated on stiff and 2000 cells/well were plated on soft hydrogels.

3.1.2 Cryopreservation of Cells

Cells of 80-90 % confluency were gently detached from the plate using Trypsin–EDTA and subsequently resuspended in PBS. Next, the cell suspensions were transferred into 15 ml conical tubes and centrifuged for 5 minutes at 1500 rpm. The resulting cell pellets were then transferred into cryovials and stored in liquid nitrogen tanks after resuspension in a freezing solution composed of 90% FBS and 10% dimethyl sulfoxide (DMSO).

3.2 Fabrication of Polyacrylamide Hydrogels

To synthesize polyacrylamide hydrogels, a previously established protocol was followed (Barber-Pérez et al., 2020). To investigate the effects of substrate stiffness on growth, morphology, and response to treatment of cancer cells, we fabricated polyacrylamide hydrogels with Young's moduli ranging from 0.5 to 22 kPa. These conditions closely resemble the physiological properties of healthy human lung tissue, which exhibits low stiffness, in comparison to the elevated stiffness of cancerous lung tissue.

At first, 35 mm glass-bottom dishes (Cellvis, D35-14-1-N) or 24-well glass bottom plates (Cellvis, P24-1.5H-N) were treated with Bind-Silane solution for 30 minutes at room temperature to enhance hydrogel adherence to the glass-bottom surface. This solution contains 3-(Trimethoxysilyl)propyl methacrylate (Thermo Scientific, cat. no. 216555000), along with acetic acid and absolute ethanol (96% by volume). Following the aspiration of Bind-Silane, the glass was rinsed twice with 96% ethanol by volume and allowed to air dry. For hydrogel preparation, a mixture of 40% (w/v) acrylamide (Sigma-Aldrich, A4058) and 2% (w/v) N, N-methylene-bis-acrylamide (Thermo scientific, J63265.AP) was combined with PBS (***Figure 13***). Distinct pre-polymer solutions were prepared, corresponding to the Elastic moduli shown in ***Table 2***.

Table 2. *Relative acrylamide and bis-acrylamide concentrations for the fabrication of hydrogels with different stiffness.*

AA 40% (ul)	AA-%	BisA 2% (ul)	BisA-%	PBS (ul)	Elastic Modulus (~kPa)
63	5	10	0.04	397	0.5
63	5	17.5	0.07	365	2
63	5	25.2	0.1	416	3.15
63	5	37.8	0.15	403	4.47
94	7.5	50	0.2	356	9.6
150	12	50	0.2	300	22

The polymerization of polyacrylamide was initiated by adding N,N,N′,N′-tetramethylethylenediamine (TEMED) (0.2% by volume, Thermo Fisher Bioreagents, BP150-100) along with 10% ammonium persulfate (APS) (0.1% by volume, Thermo Fisher Bioreagents, 327081000) to the solution. After this, the polymerizing solution was gently mixed to minimize the incorporation of oxygen, and a 15 ul droplet was placed on the glass bottom. A round coverslip with a diameter of 13 mm was then placed over the droplets to promote their spreading, leading to the creation of a uniform hydrogel. The hydrogels were then allowed to polymerize at room temperature for 30 minutes, and the plates were sealed with parafilm to block any oxygen from interfering with the polymerization. Once the polymerization process was complete, the gels were immersed in PBS and kept at 4°C overnight in order to reach swelling equilibrium. The following day, the coverslips were carefully removed using medical tweezers and a bent needle, and the gels were washed twice with PBS to remove any unpolymerized acrylamide.

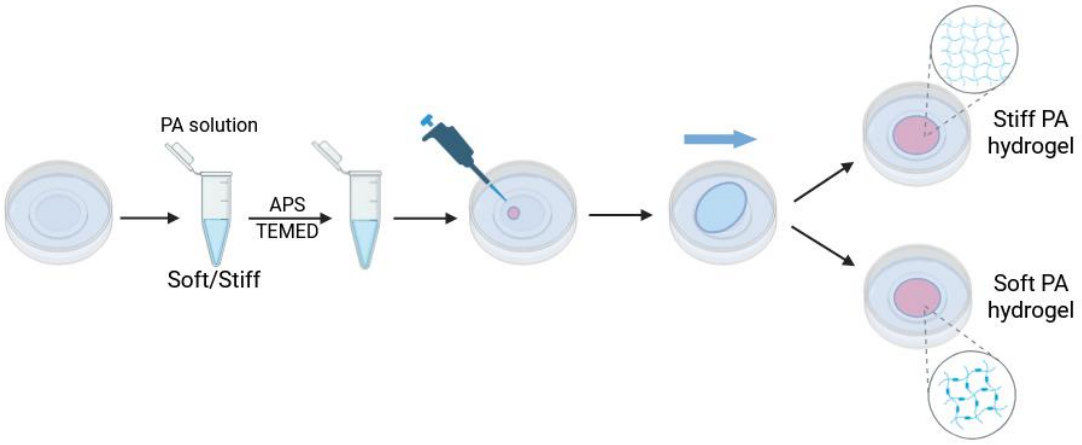

Figure 13. *Schematic representation of the steps for the creation of polyacrylamide hydrogels. Following mixing the PBS with acrylamide (AA), and bis-acrylamide (BisA), the polymerizing agents APS and TEMED are added and the solution is carefully pipetted. 15 ul of the started mixture is pipetted close to the edge of the well. The coverslip is placed as illustrated in the figure and the system is left undisturbed until hydrogel polymerization is complete (Figure created by Biorender.com)*

3.3 Morphological Analysis

For these experiments, 2500 cells/well (for PC9, HCC827 and HCC4006) were seeded on Easy Coat™ hydrogels bound to 96 well plates with a black polystyrene frame and #1.5 (0.16 - 0.19 mm thick) borosilicate glass (Matrigen). The plate contains 8 replicates of 0.1, 0.2, 0.5, 2, 4, 8, 12, 25 and 100 kPa hydrogels. The next day cells were fixed with 4% paraformaldehyde (PFA) for 20 minutes, permeabilized with 0.3% Triton X-100 in PBS for 10 minutes and stained with Hoechst 33342 (Sigma-Aldrich, B2261) and 1:500 Phalloidin-Atto 565 (Sigma-Aldrich, 94072) in PBS for 1h in the dark. After incubation, the staining solution was aspirated, and cells were washed three times very gently with PBS. Cells were then kept in PBS at 4^{o}C until imaging.

Images of single cells from random positions across each hydrogel were captured using a Nikon AX confocal microscope system (CFI Apochromat LWD Lambda S 40XC WI), and 594 nm and 342 nm laser lines, with Nyquist sampling set to 3.5 nm zoom. Z-stacks of the cytoskeleton of each cell were acquired. Cell area (μm^2) and circularity (a.u.) were quantified using ImageJ/Fiji software. First, maximum intensity projection was performed in all stacks. Then, cell outlines were segmented via the threshold tool, selected with the wand tracing tool, and cataloged in the ROI manager to measure area and perimeter, with data exported to an .xlsx file. Circularity was determined using the formula 4π*area/$(perimeter)^2$ where a value of 1 denotes a perfect circle and values approaching 0 indicate increasingly elongated morphologies.

3.3.1 Statistical Analysis

All statistical analysis were performed in GraphPad Prism 8.4.2. Statistical significance between multiple groups was determined using one-way ANOVA. All results are from three independent experiments unless stated otherwise. For morphological characterizations at least 40 single cells were analyzed per condition. Cell proliferation was monitored as percentage confluency over time using the IncuCyte® Zoom live-cell imaging system. Growth kinetics were analyzed by nonlinear regression using a logistic growth model. To compare proliferation between conditions, a global curve-fitting approach was applied, and differences between models were evaluated using

the extra sum-of-squares F test. For all analyses p values < 0.05 were considered significant. Error bars are represented as mean ± SEM. GraphPad Prism 8.4.2 was used for all statistical analysis and graphs.

3.4 Analysis of Cell Confluency

For these experiments, 25000 cells/well for all cell lines were seeded on soft and stiff hydrogels (24-well plate). After cell seeding, the plates were placed into IncuCyte® Zoom System (objective 10x, 4 pictures/well) and their growth was followed for 5 days. Automated image analysis was conducted using IncuCyte® Analysis Software, which utilized a specialized Phase Object Masking tool. This software identified cellular structures by evaluating brightness and cell area in comparison to the background. For each cell line, an image stack was generated to train the software to differentiate cells from the background. Filter parameters, including segmentation and area, were optimized for each cell line to enhance the accuracy of cell detection and minimize the misidentification of small impurities as cells. Then the software calculated the percentage of surface area which was covered by cells over time. These data were then used to generate growth curves and to evaluate the impact of substrate stiffness on cell proliferation.

3.5 Dose response experiments

3.5.1 Drug treatment

EGFR-driven NSCLC cell lines were treated with the EGFR inhibitor osimertinib (HY-15772, MedChemExpress). A stock solution was prepared at a concentration of 10mM in DMSO. From this, several additional stock concentrations were prepared. The concentration range needed for each experiment differed mainly depending on the specific cell line being studied and the rationale of each experiment. Each final concentration was prepared in fresh full medium at a ratio of 1:1000 before application. 0.1 % DMSO (Sigma-Aldrich) was used as a control.

3.5.2 Analysis of number of cells

For these experiments, 4000 cells/well (HCC827), 2500 cells/well (HCC4006) and 3000 cells/well (PC9) were seeded on plastic (96-well plate), 75000 cells/well (HCC827), 40000 cells/well (HCC4006) were seeded on stiff and 75000 cells/well (HCC827), 50000 cells/well (HCC4006) were seeded on soft hydrogels (24-well plate). Also, for PC9 1500 cells/well were plated on stiff and 2000 cells/well were plated on soft hydrogels (Matrigel, HTP plates). All cell lines were treated with Osimertinib or DMSO for 3 days. Then cells were fixed with 4% PFA for 20 minutes at room

temperature, rinsed three times with PBS and stained with 1 ug/ml Hoechst 33342 in the dark for 30 minutes at room temperature. Upon completion of the incubation, the cells were washed four times with PBS. Nuclei were imaged using Leica AF 7000 microscope, 10x HC PL FLUOTAR lens with NA 0.30 and an A UV filter (BP340-380 400 LP 425).

The analysis of the acquired microscopy data was conducted with ImageJ, Fiji software. First, background subtraction was performed to remove low-intensity details and the background. Thresholds were then adjusted to distinguish cell nuclei which were segmented with Hoechst 33342 from the surrounding background, ensuring clear detectability. Next, the watershed tool separated overlapping nuclei that thresholding had merged into single objects. Segmented images were analyzed using the Analyze Particles function to collect quantitative data; size parameters were set to 50–1500 pixels to exclude noise and ensure accurate measurements. Nuclei counts per well were normalized to the average DMSO value for each stiffness condition in Microsoft Excel, and dose response curves were generated using GraphPad Prism 8.4.2 software for Windows. Although experimental drug concentrations were administered in nanomolar (nM), all values were converted to picomolar (pM) prior to analysis to facilitate logarithmic transformation *(X = log (concentration in pM)*. The IC_{50} values were then determined with nonlinear regression analysis using the *log(inhibitor) vs. response – Variable slope (four parameters)* -equation *(Y=Bottom + (Top-Bottom)/(1+10^((LogIC50-X) *HillSlope).*

4. Results

4.1. NSCLC cell lines are mechanoresponsive

First, we aimed to investigate whether NSCLC cells with EGFR mutations are mechanoresponsive. We thus studied whether and how does the morphology of those cells alter in response to matrix stiffness. We used three human NSCLC cell lines with EGFR mutations (see ***Table 1***), namely PC9, HCC827 and HCC4006, and plated them on custom made polyacrylamide hydrogels (Matrigen) in 96 well plates with #1.5 glass bottom, suitable for microscopy. The hydrogels spanned a wide range of matrix stiffness: 0.1, 0.2, 0.5, 2, 4, 8, 12, 25, 100 kPa as well as glass and were coated with collagen I, the most common ECM protein in the lung (Gaggar & Weathington, 2016). Cells were plated sparsely and the cell area and circularity of single cells were analyzed using the actin marker phalloidin. For each condition at least 40 cells were analyzed in total from 3 independent experiments. We found that all three cell lines are mechanoresponsive, meaning they respond to matrix stiffness by altering their morphology. They adopt a smaller and rounder shape on softer matrices and are larger and more spread on stiffer matrices (***Figures 14-16***).

Importantly, by using this wide range of matrix stiffness we could not only explore the correlation between stiffness and morphological changes, but we could also identify the stiffness in which the differences are more pronounced. We found that all cell lines perceived substrates up to 0.5 - 1 kPa as soft, whereas they become more spread and less circular when stiffness is above 2 kPa, a stiffness which is typically considered very soft for normal cells. Interestingly, whereas PC9 and HCC827 cells show no significant changes in their morphology beyond 2 kPa (***Figure 14 and 15***), HCC4006 cells exhibit more gradual responses with further morphological changes in response to increasing stiffness (***Figure 16***).

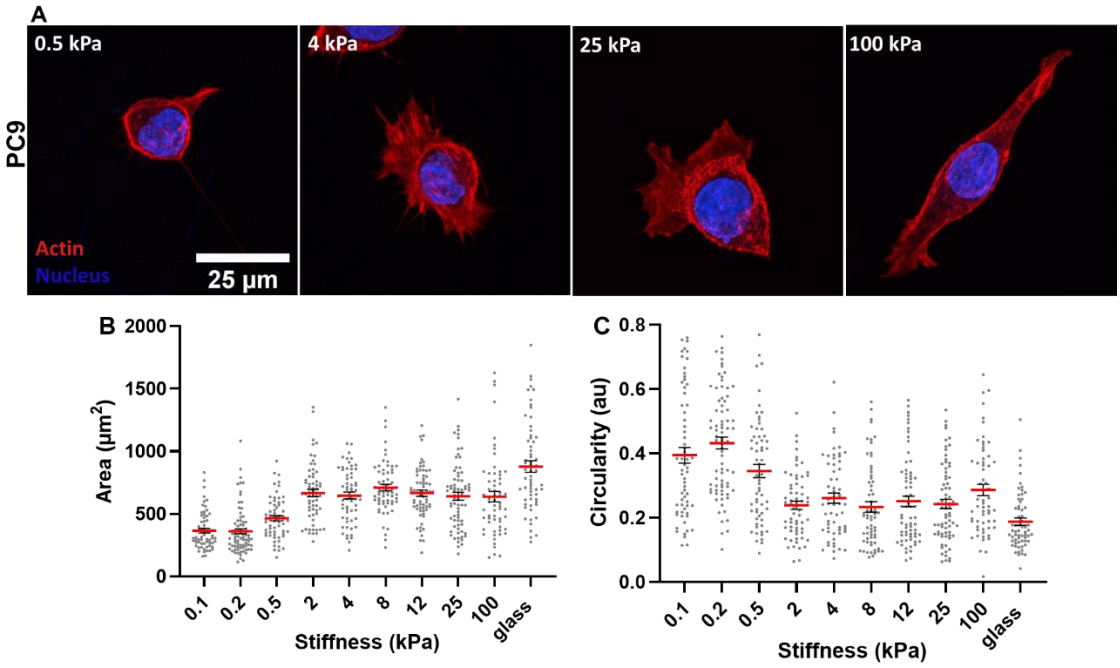

Figure 14. *PC9 cells are mechanoresponsive, as the cell area increases and the cell circularity decreases in response to increased matrix stiffness. (A) Representative confocal images of PC9 cells cultured on hydrogels with various stiffness levels for 24h and stained for the actin marker phalloidin (red) and the nuclear marker Hoechst (blue). Images are maximum intensity projection. (B, C) Quantification of the cell area (B) and cell circularity (C). Data are means ±SEM.; n > 40 cells from three repeats; P<0.0001(one-way ANOVA) (95 % confidence interval). au: arbitrary units.*

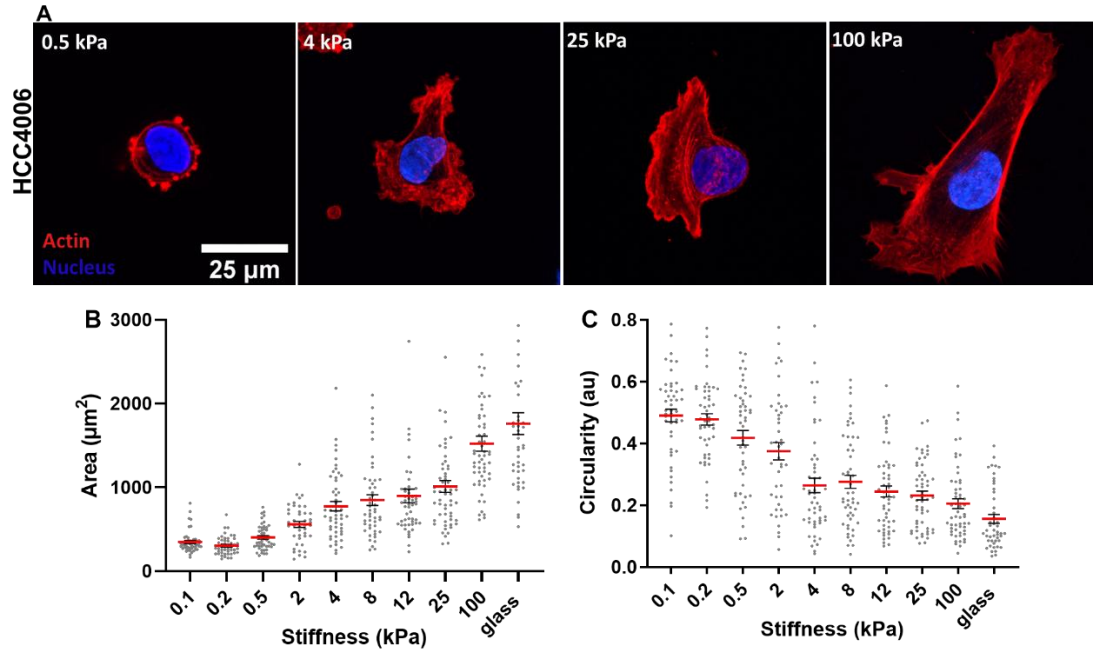

Figure 15. *HCC4006 cells are mechanoresponsive, as the cell area increases and the cell circularity decreases in response to increased matrix stiffness. (A) Representative confocal images of HCC4006 cells cultured on hydrogels with various stiffness levels for 24h and stained for the actin marker phalloidin (red) and the nuclear marker Hoechst (blue). Images are maximum intensity projection. (B, C) Quantification of the cell area (B) and cell circularity (C). Data are means ±SEM.; n > 40 cells from three repeats; P<0.0001(one-way ANOVA) (95 % confidence interval). au: arbitrary units*

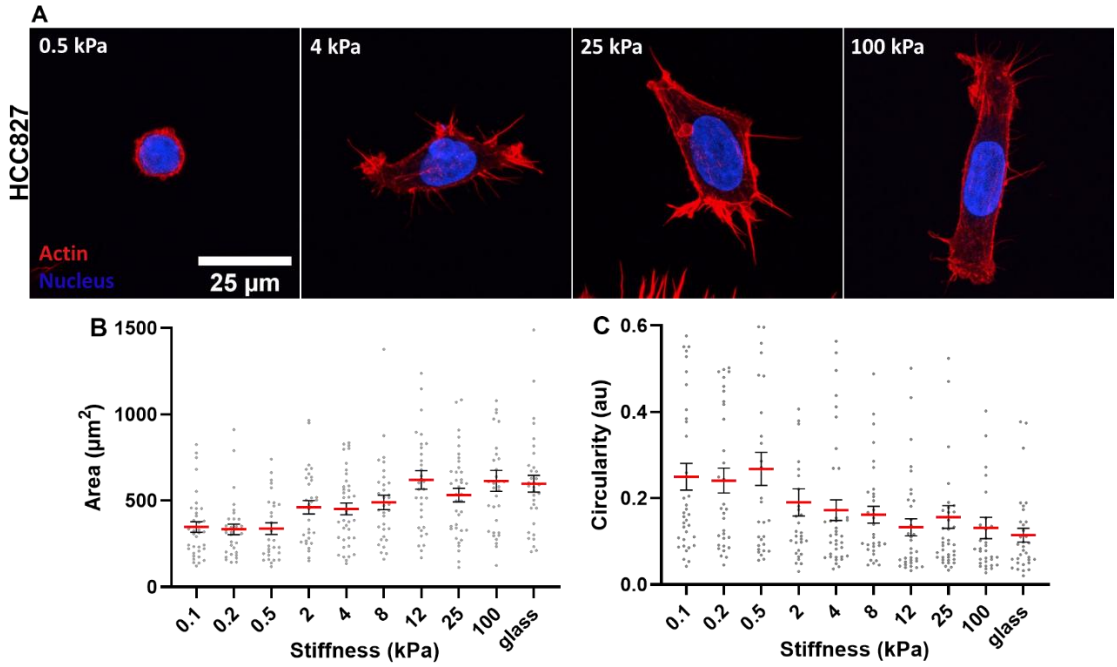

Figure 16. *HCC827 cells are mechanoresponsive, as the cell area increases and the cell circularity decreases in response to increased matrix stiffness. (A) Representative confocal images of HCC827 cells cultured on hydrogels with various stiffness levels for 24h and stained for the actin marker phalloidin (red) and the nuclear marker Hoechst (blue). Images are maximum intensity projection. (B, C) Quantification of the cell area (B) and cell circularity (C). Data are means ±SEM.; n > 30 cells from three repeats; P<0.0001(one-way ANOVA) P<0.0001(one-way ANOVA) (95 % confidence interval). au: arbitrary units*

4.2. Evaluation of in-house-fabricated hydrogels

We established the fabrication of polyacrylamide (PA) hydrogels with tunable stiffness in our laboratory following a previously published protocol established by Dr Georgiadou (Barber-Pérez et al., 2020). In that study, human telomerase-immortalized fibroblasts (TIFs) were shown to be mechanoresponsive, as when cultured on PA hydrogels with a stiffness gradient, TIFs increased their cell spreading and adhesion length in response to substrate stiffness up to approximately 7 kPa, whereas no further changes were observed at higher stiffness values, indicating that the substrate was perceived as stiff (Barber-Pérez et al., 2020). Based on these findings, we assessed the mechanoresponsiveness of TIFs on our in-house-fabricated hydrogels to validate that the hydrogels exhibit the expected mechanical behavior.

We fabricated PA hydrogels on glass-bottom dishes with defined stiffness values of 0.5, 2, 3.15, 4.47, 9.6, and 22 kPa, following established protocols (Barber-Pérez et al., 2020). TIFs were seeded onto the hydrogels and cultured for 24 h, after which changes in cell area and circularity were quantified as readouts of mechanoresponsiveness. TIFs cultured on the softest substrate (0.5 kPa) exhibited the smallest cell area and the highest circularity (***Figure 17***). With increasing substrate stiffness (2 - 4.47 kPa), cells progressively increased their spreading area and adopted a less rounded morphology (***Figure 17***). In contrast, no further changes in cell area or circularity were observed on stiffer hydrogels (≥4.47 kPa), indicating a plateau in the cellular response to stiffness (***Figure 17B*** and ***C***). These results demonstrate that the in-house-fabricated hydrogels recapitulate the mechanoresponsive behavior reported previously, consistent with the published observations (Barber-Pérez et al., 2020).

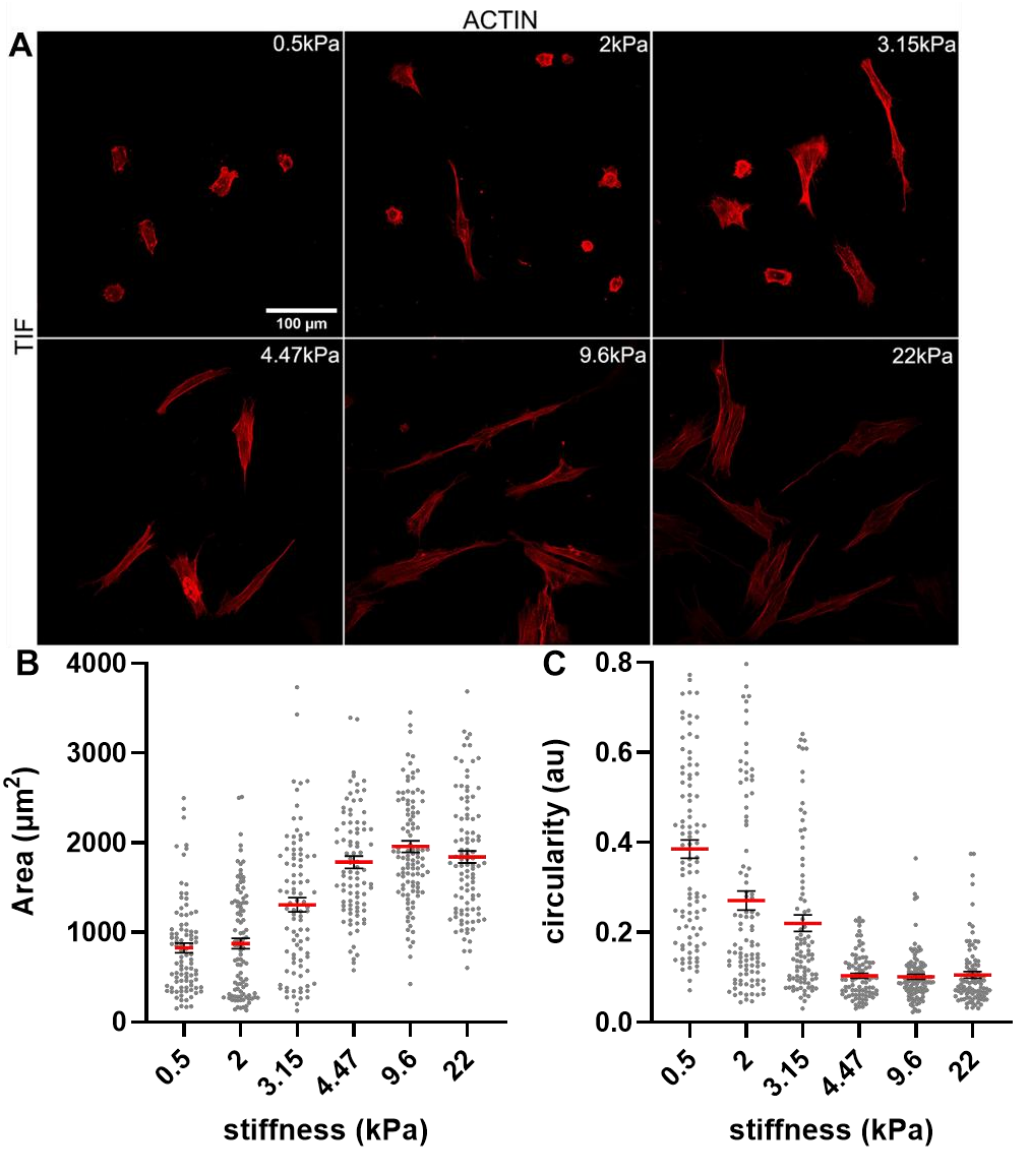

Figure 17. *Cell area and circularity of TIF cells cultured on 0.5kPa, 2kPa, 3.15kPa, 4.47kPa, 9.6kPa and 22kPa hydrogels A. Representative max intensity projection images of actin-stained cells. Images taken using Nikon AX confocal microscope system. A water immersed 40x objective lens was used. B-C. Statistical analysis of cell area (B) and circularity (C) Max intensity projection images were used for data acqurement via ImageJ. Data are means ±SEM.; n > 80 cells from two independent experiments (****, P<0.0001), au: arbitrary units.*

4.3. ECM stiffness increases cell growth

As shown above, all three EGFR-driven NSCLC cell lines (PC9, HCC827 and HCC4006) are responsive to mechanical cues by altering their cell morphology. Here, we used our in-house fabricated hydrogels to study the impact of stiffness on cell growth. More specifically, we seeded the cells on soft (0.5 kPa) hydrogels, representing the normal lung stiffness, and stiff (22 kPa) hydrogels, representing the cancerous, fibrotic lung stiffness, and assessed their growth over time by live cell imaging with IncuCyte® Zoom.

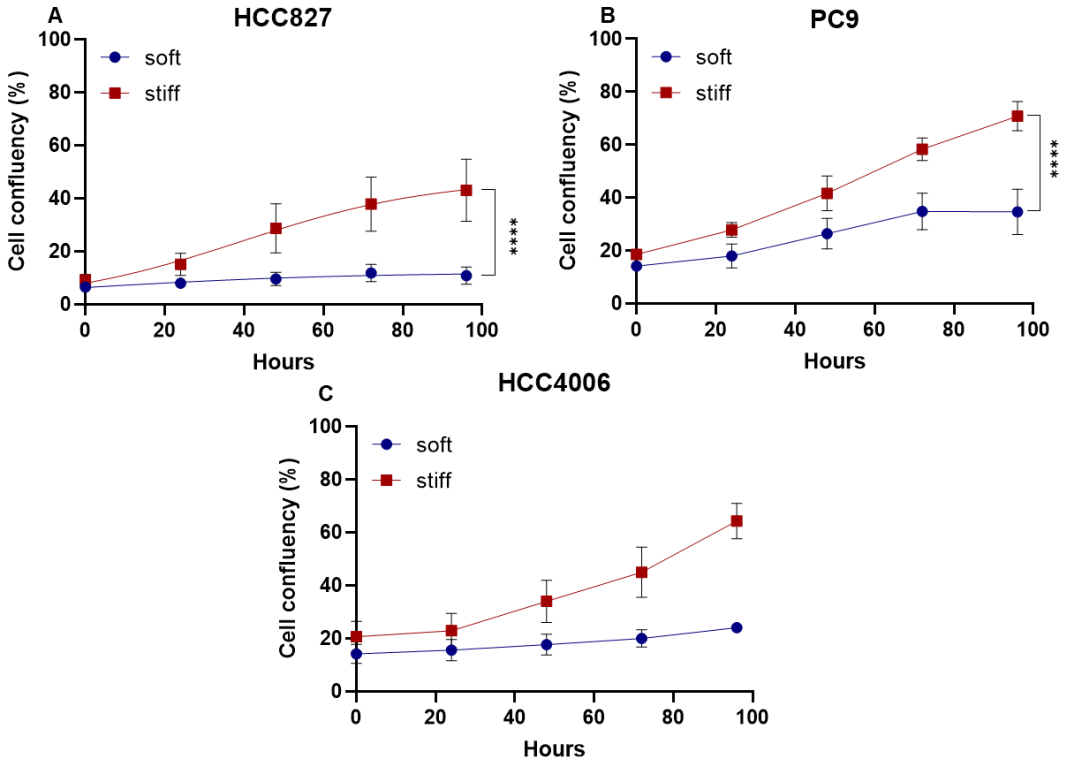

Figure 18. *Confluency HCC827 (A), PC9 (B), and HCC4006 (C) cells growing on soft and stiff substrates overtime. Growth curves representing the percentage of surface area occupied by cells on soft (blue line) and stiff (red line) substrates were generated using non-linear regression following a logistic growth model to fit the confluency data. Data are presented as means ±SEM.; n = 3 independent experiments for HCC827 and PC9 cell lines; n = 1 experiment for HCC4006 cell line.*

As shown in ***Figure 18***, we observed significant differences in the growth of cells cultured on soft compared to stiff substrates across all three NSCLC cell lines, with cells on soft matrix growing significantly slower than on stiff matrix. It is noteworthy that cells do not grow at all (HCC827, HCC4006) or very minimally (PC9) on soft matrix over time. In addition, HCC827 and HCC4006 cells on soft matrix seem to grow overtime in spheres (***Figure 19***), making it hard to assess their confluency (phase

contrast, area covered by cells). Collectively, these findings suggest that increased ECM stiffness enhances non-small cell lung cancer (NSCLC) cell proliferation over time.

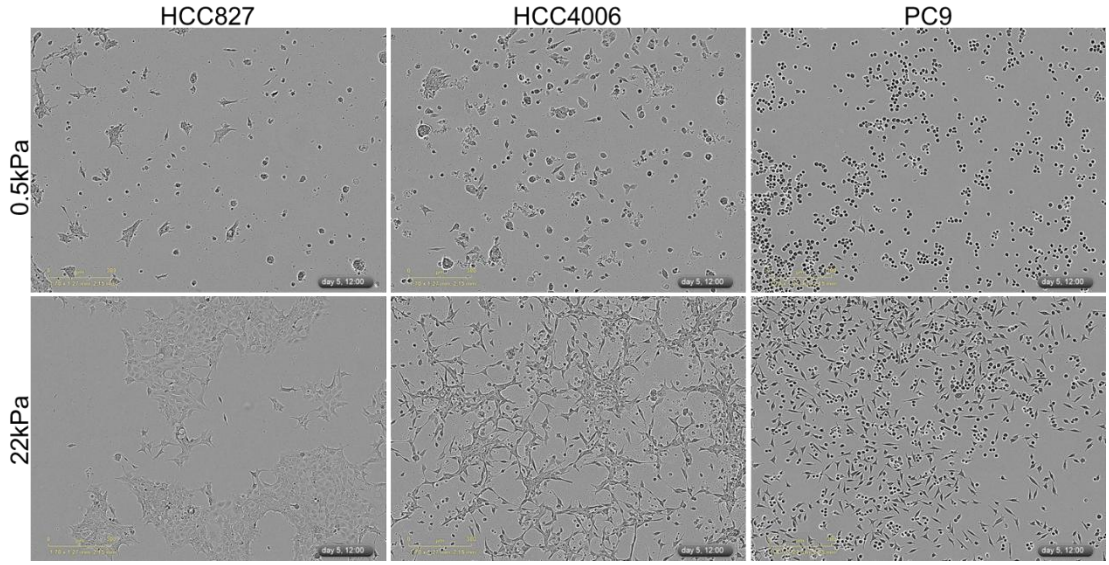

Figure 19. *Representative Phase-Contrast images from IncuCyte Zoom system of PC9, HCC827 and HCC4006 cell line on day 5.*

4.4 ECM stiffness differentially regulates the response of cells to Osimertinib treatment

Next, we wanted to study whether matrix stiffness affects the sensitivity of lung cancer cells to drug treatment. Given that all the three cell lines have EGFR mutations (***Table 1***) we studied their response to the EGFR inhibitor Osimertinib. Although the sensitivity of those cell lines to Osimertinib in standard cell culture conditions (plastic) is well known, we decided to first confirm it in our cells and use it as a reference for subsequent experiments. Therefore, dose-response assays were performed using a broad range of osimertinib concentrations (1 nM - 10 uM), with logarithmically spaced intermediate doses, to accurately determine drug sensitivity and quantified the number of Hoechst 33342-stained nuclei at the end of the experiment.

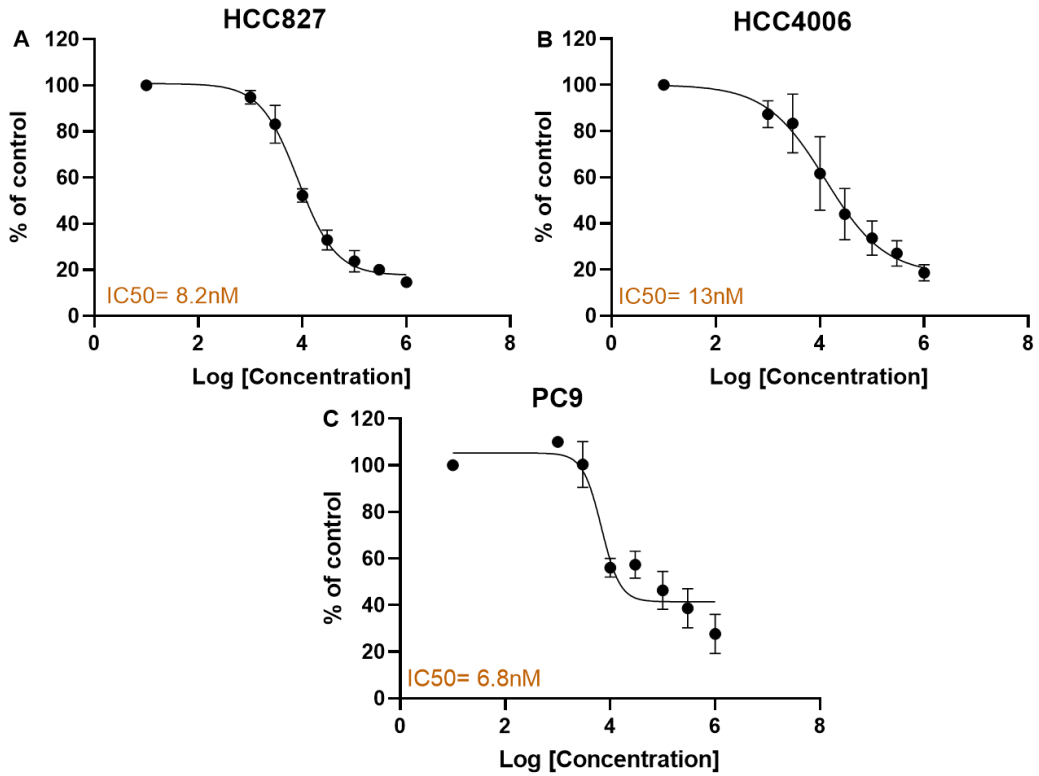

Figure 20. *Sensitivity of HCC4006, HCC827 and PC9 cells to Osimertinib. Dose response curves of HCC827 (A), HCC4006 (B) and PC9 (C) cells grown on plastic substrates. While the drug was administered in nM, the X-axis represents the concentration in pM to optimize the curve-fitting algorithm and calculation. Data points represent the mean ± SEM. The IC_{50} values (expressed in nM in the graphs) were derived from the four-parameter variable slope equation shown in the Methods. n = 3 independent experiments for all cell lines.*

Cell proliferation following osimertinib treatment on tissue-culture plastic was assessed in HCC827, HCC4006 and PC9 cells. In our hands, the IC_{50} of osimertinib for cells grown on plastic was determined to be *8.2 nM* for *HCC827* (***Figure 20A***), 13 nM for HCC4006 (***Figure 20B***) and 6.8 nM for PC9 (***Figure 20C***). While the main focus is the IC_{50} of osimertinib in soft and stiff substrates, evaluating its effect on plastic is also important. This evaluation establishes baseline for drug activity and supports further research on its effects in cells grown on soft and stiff hydrogels.

We further assessed the IC_{50} of osimertinib for the same cell lines cultured on either soft or stiff matrices in order to evaluate the impact of matrix stiffness on cellular responses to osimertinib treatment. Given the technical constraints associated with PA hydrogels and the fact that they are fabricated in 24-well plates, we reduced the number of drug concentrations tested to five, focusing on a range from 1 nM to 1 uM with logarithmically spaced intermediate concentrations. In addition, in *HCC827* cells

the IC_{50} was *3 nM* on stiff and *2.8 nM* on soft hydrogels (***Figure 21A***), demonstrating high sensitivity to Osimertinib across both matrix stiffnesses. *HCC4006* cells demonstrated an IC_{50} of *5.8 nM* on stiff hydrogels and *3.1 nM* on soft hydrogels (***Figure 21B***), suggesting that cells on soft substrates were approximately twice as sensitive. In PC9 cells, the IC_{50} for the cells growing on stiff hydrogels was *60.3 nM* and on soft hydrogels *26.5 nM* (***Figure 21C***), indicating a threefold increase in sensitivity on soft substrates compared to stiff ones. These results further support that matrix rigidity significantly affects drug sensitivity in specific EGFR-mutant lung cancer cell lines.

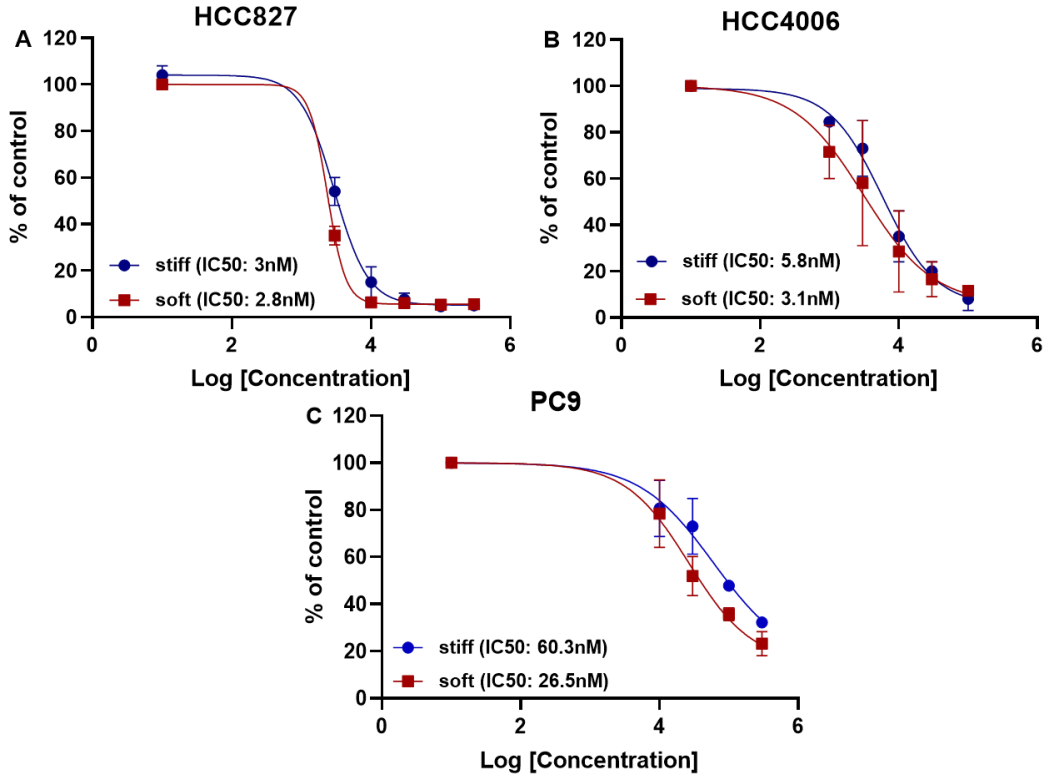

Figure 21. *Sensitivity of HCC4006, HCC827 and PC9 cells to Osimertinib. Dose response curves of HCC827 (A), HCC4006 (B) and PC9 (C) cells grow on soft and stiff PA hydrogels. While the drug was administered in nM, the X-axis represents the concentration in pM to optimize the curve-fitting algorithm and calculation. Data points represent the mean ± SEM. The IC_{50} values (expressed in nM in the graphs) were derived from the four-parameter variable slope equation shown in the Methods. n = 3 independent experiments for PC9 and HCC827; n = 2 independent experiments for HCC4006.*

In ***Figure 22***, we show representative images of cells (HCC827, HCC4006 and PC9) on soft (0.5kPa) and stiff (22kPa) matrix at the end of the treatment (3 days with DMSO or the indicated concentration of Osimertinib). At 10 nM, which exceeds the IC_{50} for both conditions for HCC827 and HCC4006, cell viability was strongly inhibited

regardless of substrate stiffness. In PC9 cells (Figure 21C and 22C), a 30 nM dose, inhibited cell viability on the soft substrate but not on the stiff one.

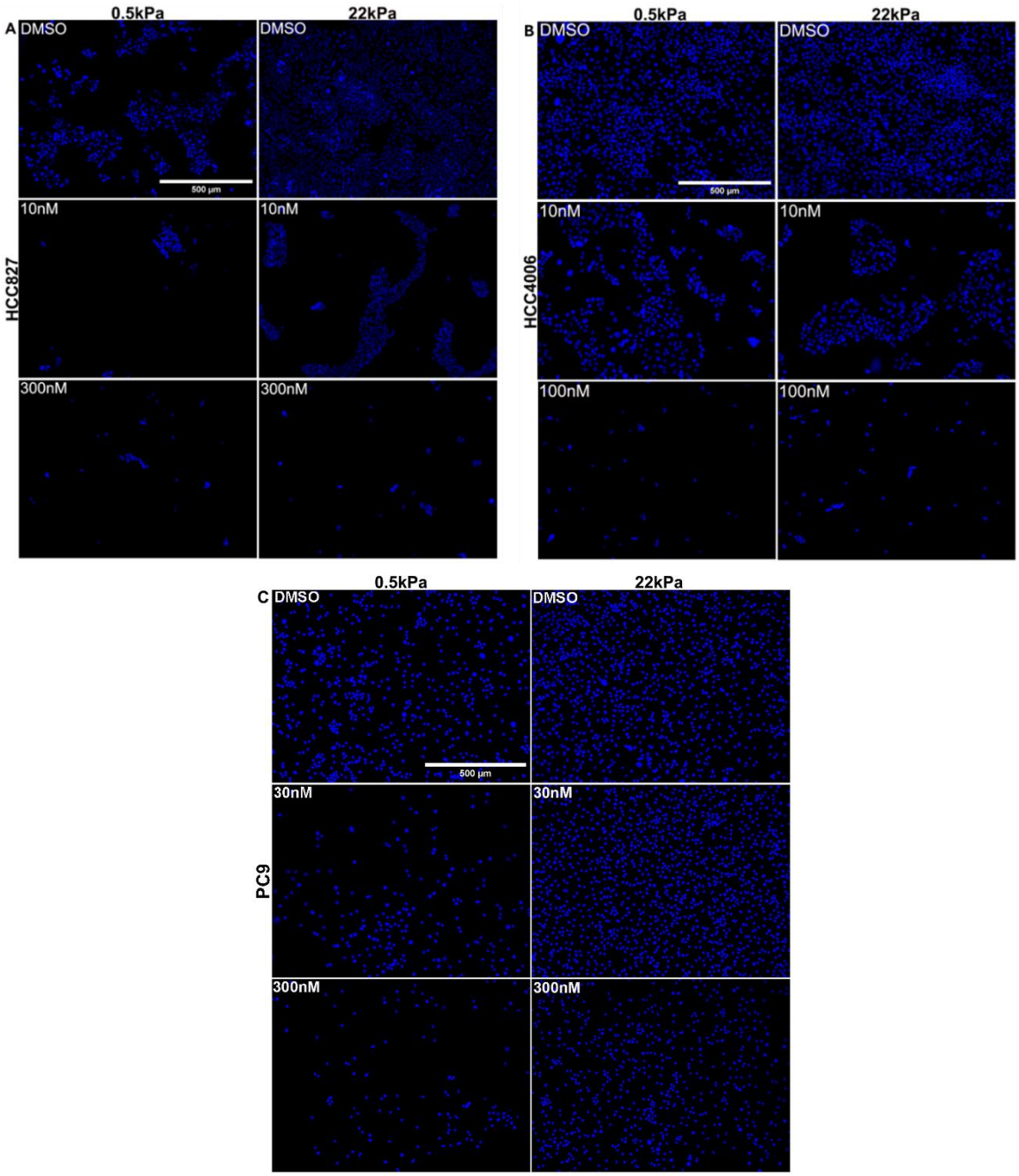

***Figure 22**. Representative images of nuclei of HCC827 (A), HCC4006 (B) and PC9 (C) cells at the end of the experiment shown in Figure 21. Images were obtained using a Leica AF7000 microscope with a 10x HC PL FLUOTAR lens (NA 0.30).*

5. Discussion

5.1. Conclusions

This thesis examines the critical role of matrix stiffness, a biomechanical characteristic of tumor microenvironment, in modulating the behavior and therapeutic response of EGFR-mutated lung cancer cells. Polyacrylamide hydrogels functionalized with Collagen Type I were employed to recapitulate the stiffness of lung tissue, spanning from physiological softness to the pathological rigidity observed in lung adenocarcinoma.

To study how ECM stiffness shapes cancer cell morphology, growth, and treatment response, we fabricated polyacrylamide hydrogels with a tunable stiffness according to a previously published protocol (Barber-Pérez et al., 2020). These hydrogels are easy and quick to make in any lab, require no special equipment, and are inexpensive. Also, their round shape (12 mm diameter) and thin size (about 80–100 μm) are well suited for high-resolution imaging. A key advantage of these polyacrylamide hydrogels is that they allow precise control of matrix stiffness, making them valuable tools for studying cancer cell-matrix interactions.

In Barber-Pérez et al., 2020, the mechanoresponsiveness of the fibroblast line, TIFs, was characterized using stiffness-tunable hydrogels. To validate that the hydrogels fabricated in-house exhibited the expected mechanical properties, we assessed the mechanoresponsive behavior of TIF cells on our hydrogels. Phalloidin staining revealed that on soft substrates (0.5–2 kPa), TIF cells exhibited a smaller, rounded morphology with minimal spreading. On intermediate-stiffness substrates (3.15-4.47kPa), cells began to spread more and increase in cell area. In contrast, on stiff substrates (9.6-22kPa), these cells showed increased surface area and significant spreading. These observations are in-line with the findings reported by (Barber-Pérez et al., 2020), confirming that our hydrogel fabrication reproduces the published protocol and yields substrates with the expected biomechanical behavior.

Next, we evaluated the response of lung cancer cells to substrate stiffness, particularly their morphology and their proliferative behavior. Using three EGFR-mutant NSCLC cell lines (PC9, HCC4006, and HCC827), we found that all three are highly sensitive to matrix rigidity and they respond by altering their cell shape and spreading. On very soft substrates (0.1-0.5kPa) NSCLC cells appear to be smaller and more rounded (observed through phalloidin staining), whereas on stiffer substrates (≥2 kPa) they adopt a larger, more spread phenotype with increased protrusions. In accordance to our findings, it has been shown that lung adenocarcinoma cells acquire a more spread

shape when cultured on stiffer substrates (Alonso-Nocelo et al., 2018; Park et al., 2024).

We have also found that all three NSCLC cell lines exhibited a pronounced morphological transition between 0.5 kPa and 2 kPa. Importantly, PC9 and HCC827 cells reached a morphological plateau at 2 kPa, with no further increases in cell area observed at higher stiffnesses (up to 100 kPa and glass). In contrast, HCC4006 cells displayed a more graded response, continuing to increase their cell area with increasing substrate stiffness. These findings indicate that while all three EGFR-mutant NSCLC cell lines are highly mechanosensitive, they differ in how they integrate increasing mechanical cues.

The observation that 2 kPa is perceived as a stiff environment by EGFR-mutant NSCLC cells contrasts with the prevailing data in mechanobiology. In many cell models, stiffness values around 2 kPa are widely perceived as soft. For instance, HeLa cells and TIFs exhibit soft-state morphology on hydrogels with stiffness values of ~2kPa (Barber-Pérez et al., 2020), a behavior that we also observed for TIFs in our own experiments (***Figure 17B***). Similarly, mouse embryonic fibroblasts (MEFs) and human breast myoepithelial cells maintain a rounded, non-spread morphology at 2 kPa (Andreu et al., 2022; Elosegui-Artola et al., 2014). Moreover, in primary human colon tumor cells, 2 kPa gels represent the soft condition when compared with substrates of 10 kPa or higher (Cambria et al., 2024). Additionally, MDA-MB-231 breast cancer cells exhibited lower spreading and increased circularity on hydrogels of ~1kPa (Syed et al., 2017).

Thus, the pronounced sensitivity of EGFR-mutant NSCLC cells to relatively low stiffness values suggests that these cells may possess an intrinsic sensitivity to mechanical forces. One possible explanation is that oncogenic EGFR signaling alters cytoskeletal organization, focal adhesion dynamics or mechanotransduction pathways, thereby lowering the threshold at which cells interpret their mechanical environment as stiff. Alternatively, downstream programs associated with EGFR signaling, such as EMT and YAP/TAZ activation, may prone cells to respond robustly to modest increases in matrix rigidity.

To further understand this sensitivity, future studies should compare EGFR-mutant NSCLC cell lines with lung cancer models driven by alternative oncogenic mutations, such as KRAS, ALK, or MET. Additionally, using isogenic models with or without mutant EGFR, or with controlled EGFR expression on substrates of defined stiffness, may help determine whether EGFR or downstream processes influence this enhanced

mechanosensitivity. Such approaches would help clarify whether the perception of 2 kPa as a stiff microenvironment represents a broader feature of EGFR-driven lung cancer or a more general consequence of oncogenic signaling.

Across all cell lines, cell growth was significantly higher on stiff hydrogels compared to soft ones. This result aligns with previous studies, including some focusing on lung cancer, showing that ECM stiffness accelerated growth on stiffer substrates (Ishihara et al., 2013; Park et al., 2024). While traditional models attribute growth primarily to genetic mutations, the present results suggest that mechanical tension can also amplify oncogenic signaling (Liang & Song, 2023).

In this thesis, cell growth was evaluated based on cell confluency using the IncuCyte® Zoom Analysis Software. Although this approach allows continuous, non-invasive monitoring of cell growth over time, it has limitations when applied to stiffness-tunable hydrogels. On soft hydrogels, the cells tend to be smaller and often form spheres, as seen in HCC827 and HCC4006 cells (***Figure 19***), thus, confluency measurements can underestimate true cell numbers or proliferative activity, even when cell cycle progression is comparable to that on stiffer substrates. Also, hydrogels can vary in how clear they are, bend light differently, and add background texture. Therefore, to get a more accurate picture, future work should combine confluency measurements with more direct proliferation assays, such as Ki-67 immunostaining on fixed gels or ATP-based viability assays, to provide a more robust assessment of proliferation.

Further, the response of lung cancer cells to osimertinib treatment was assessed in cells growing on either soft or stiff matrix. Initially, we determined the IC_{50} values of osimertinib for HCC827, HCC4006 and PC9 cell lines cultured as standard monolayers on plastic. The values obtained were consistent with previously published reports and pharmacogenomic datasets. Indeed, for *HCC827* cell line we estimated an *IC_{50} of 8.2 nM* when in the literature it ranges between ~ 10 - 43 nM (Chen et al., 2023; Lategahn et al., 2019), and the Genomics of Drug Sensitivity in Cancer (GDSC) pharmacogenomic dataset reports an IC_{50} of ~27.6 nM (https://www.cancerrxgene.org/). For the *HCC4006* cell line (*IC_{50}= 13 nM*), reported IC_{50} values for osimertinib approximately 20–40 nM (Furukawa et al., 2021). For the *PC9* cell line (*IC_{50}= 6.8 nM*), reported IC_{50} values for osimertinib are reported again between 20–40 nM (Furukawa et al., 2021; Masuzawa et al., 2017). These results validated our experimental conditions and provided a reference point for subsequent experiments on physiologically relevant substrates.

When osimertinib sensitivity was assessed on soft and stiff hydrogels, distinct stiffness-dependent responses emerged. The HCC827 cell line demonstrated comparable response to Osimertinib (IC_{50} of 3 nM on stiff and 2.8 nM on soft hydrogels) across substrate stiffnesses. Similarly, exhibited only modest differences between conditions, with IC_{50} values of 5.8 nM on stiff and 3.2 nM on soft hydrogels. PC9 cells though exhibited a greater difference in drug response, with an IC_{50} of 60.3 nM on stiff compared to 26.5 nM on soft substrates. This approximately threefold increase suggests that PC9 cells are more sensitive to mechanical tension and increasing matrix stiffness could impair the efficacy of EGFR inhibition.

Notably, even at high Osimertinib concentrations (300 nM), a persistent population of PC9 cells survives drug treatment across both soft and stiff substrates. This suggests that these cells possess adaptive resilience, enabling them to evade treatment-induced lethality. Understanding the mechanisms underlying cells' survival mechanisms is crucial for overcoming clinical resistance. Further exploration of the molecular mechanisms underlying this stiffness-dependent sensitivity could reveal novel therapeutic targets or strategies for patient stratification. Future studies should focus on elucidating the specific signaling pathways modulated by ECM stiffness that contribute to altered drug sensitivity.

Together, these findings point to a complex interplay between oncogenic signaling, mechanical cues, and adaptive survival mechanisms. A deeper understanding of how ECM stiffness regulates transcriptional, metabolic, and signaling programs, particularly those involving YAP/TAZ, focal adhesion signaling, and cellular metabolism, will be essential for identifying vulnerabilities that can be therapeutically exploited. Integrating transcriptomic, metabolomic, and functional perturbation approaches in stiffness-controlled systems, as well as extending these studies to more physiologically relevant 3D cultures and patient-derived models, will be critical for translating these insights into strategies that improve clinical outcomes for patients with EGFR-mutant lung cancer.

6. References

Alonso-Nocelo, M., Raimondo, T. M., Vining, K. H., López-López, R., De La Fuente, M., & Mooney, D. J. (2018). Matrix stiffness and tumor-Associated macrophages modulate epithelial to mesenchymal transition of human adenocarcinoma cells. *Biofabrication*, *10*(3). https://doi.org/10.1088/1758-5090/aaafbc

Amelia, T., Kartasasmita, R. E., Ohwada, T., & Tjahjono, D. H. (2022). Structural Insight and Development of EGFR Tyrosine Kinase Inhibitors. In *Molecules* (Vol. 27, Number 3). MDPI. https://doi.org/10.3390/molecules27030819

Andreu, I., Granero-Moya, I., Chahare, N. R., Clein, K., Molina-Jordán, M., Beedle, A. E. M., Elosegui-Artola, A., Abenza, J. F., Rossetti, L., Trepat, X., Raveh, B., & Roca-Cusachs, P. (2022). Mechanical force application to the nucleus regulates nucleocytoplasmic transport. *Nature Cell Biology*, *24*(6), 896–905. https://doi.org/10.1038/s41556-022-00927-7

Araghi, M., Mannani, R., Heidarnejad maleki, A., Hamidi, A., Rostami, S., Safa, S. H., Faramarzi, F., Khorasani, S., Alimohammadi, M., Tahmasebi, S., & Akhavan-Sigari, R. (2023). Recent advances in non-small cell lung cancer targeted therapy; an update review. In *Cancer Cell International* (Vol. 23, Number 1). BioMed Central Ltd. https://doi.org/10.1186/s12935-023-02990-y

Asati, V., Mahapatra, D. K., & Bharti, S. K. (2016). PI3K/Akt/mTOR and Ras/Raf/MEK/ERK signaling pathways inhibitors as anticancer agents: Structural and pharmacological perspectives. In *European Journal of Medicinal Chemistry* (Vol. 109, pp. 314–341). Elsevier Masson SAS. https://doi.org/10.1016/j.ejmech.2016.01.012

Ayuso-Sacido, A., Moliterno, J. A., Kratovac, S., Kapoor, G. S., O'Rourke, D. M., Holland, E. C., Garci'a-Verdugo, J. M., Roy, N. S., & Boockvar, J. A. (2010). Activated EGFR signaling increases proliferation, survival,and migration and blocks neuronal differentiation in post-natal neural stem cells. *Journal of Neuro-Oncology*, *97*(3), 323–337. https://doi.org/10.1007/s11060-009-0035-x

Barber-Pérez, N., Georgiadou, M., Guzmán, C., Isomursu, A., Hamidi, H., & Ivaska, J. (2020). *Mechano-responsiveness of fibrillar adhesions on stiffness-gradient gels*.

Berasain, C., & Avila, M. A. (2014). The EGFR signalling system in the liver: From hepatoprotection to hepatocarcinogenesis. In *Journal of Gastroenterology* (Vol. 49, Number 1, pp. 9–23). https://doi.org/10.1007/s00535-013-0907-x

Bradley, S. H., Kennedy, M. P., & Neal, R. D. (2019). Recognising lung cancer in primary care. *Advances in therapy*, *36*(1), 19-30.

Burgess, J. K., Mauad, T., Tjin, G., Karlsson, J. C., & Westergren-Thorsson, G. (2016). The extracellular matrix – the under-recognized element in lung disease? In *Journal of Pathology* (Vol. 240, Number 4, pp. 397–409). John Wiley and Sons Ltd. https://doi.org/10.1002/path.4808

Burgstaller, G., Oehrle, B., Gerckens, M., White, E. S., Schiller, H. B., & Eickelberg, O. (2017). The instructive extracellular matrix of the lung: Basic composition and alterations in chronic lung disease. In *European Respiratory Journal* (Vol. 50, Number 1). European Respiratory Society. https://doi.org/10.1183/13993003.01805-2016

Cabanos, H. F., & Hata, A. N. (2021). Emerging insights into targeted therapy-tolerant persister cells in cancer. *Cancers*, *13*(11). https://doi.org/10.3390/cancers13112666

Cacopardo, L., Guazzelli, N., Nossa, R., Mattei, G., & Ahluwalia, A. (2019). Engineering hydrogel viscoelasticity. *Journal of the Mechanical Behavior of Biomedical Materials*, *89*, 162–167. https://doi.org/10.1016/j.jmbbm.2018.09.031

Cambria, E., Coughlin, M. F., Floryan, M. A., Offeddu, G. S., Shelton, S. E., & Kamm, R. D. (2024). Linking cell mechanical memory and cancer metastasis. *Nature Reviews Cancer*, *24*(3), 216–228. https://doi.org/10.1038/s41568-023-00656-5

Chen, X., Gu, J., Huang, J., Wen, K., Zhang, G., Chen, Z., & Wang, Z. (2023). Characterization of circRNAs in established osimertinib-resistant non-small cell lung cancer cell lines. *International Journal of Molecular Medicine*, *52*(5). https://doi.org/10.3892/ijmm.2023.5305

Chen, Z., Fillmore, C. M., Hammerman, P. S., Kim, C. F., & Wong, K. K. (2014). Non-small-cell lung cancers: A heterogeneous set of diseases. In *Nature Reviews Cancer* (Vol. 14, Number 8, pp. 535–546). Nature Publishing Group. https://doi.org/10.1038/nrc3775

Chmielecki, J., Gray, J. E., Cheng, Y., Ohe, Y., Imamura, F., Cho, B. C., Lin, M. C., Majem, M., Shah, R., Rukazenkov, Y., Todd, A., Markovets, A., Barrett, J. C., Hartmaier, R. J., & Ramalingam, S. S. (2023). Candidate mechanisms of acquired resistance to first-line osimertinib in EGFR-mutated advanced non-small cell lung cancer. *Nature Communications*, *14*(1). https://doi.org/10.1038/s41467-023-35961-y

Costa, D. B., Nguyen, K. S. H., Cho, B. C., Sequist, L. V., Jackman, D. M., Riely, G. J., Yeap, B. Y., Halmos, B., Kim, J. H., Jänne, P. A., Huberman, M. S., Pao, W., Tenen, D. G., & Kobayashi, S. (2008). Effects of erlotinib in EGFR mutated non-small cell lung cancers with resistance to gefitinib. *Clinical Cancer Research*, *14*(21), 7060–7067. https://doi.org/10.1158/1078-0432.CCR-08-1455

Cox, T. R., & Erler, J. T. (2011). Remodeling and homeostasis of the extracellular matrix: Implications for fibrotic diseases and cancer. In *DMM Disease Models and Mechanisms* (Vol. 4, Number 2, pp. 165–178). https://doi.org/10.1242/dmm.004077

Crandell, P., & Stowers, R. (2023). Spatial and Temporal Control of 3D Hydrogel Viscoelasticity through Phototuning. *ACS Biomaterials Science and Engineering*, *9*(12), 6860–6869. https://doi.org/10.1021/acsbiomaterials.3c01099

Criscione, S. W., Martin, M. J., Oien, D. B., Gorthi, A., Miragaia, R. J., Zhang, J., Chen, H., Karl, D. L., Mendler, K., Markovets, A., Gagrica, S., Delpuech, O., Dry, J. R., Grondine, M., Hattersley, M. M., Urosevic, J., Floc'h, N., Drew, L., Yao, Y., & Smith, P. D. (2022). The landscape of therapeutic vulnerabilities in EGFR inhibitor osimertinib drug tolerant persister cells. *Npj Precision Oncology*, *6*(1). https://doi.org/10.1038/s41698-022-00337-w

Cross, D. A. E., Ashton, S. E., Ghiorghiu, S., Eberlein, C., Nebhan, C. A., Spitzler, P. J., Orme, J. P., Finlay, M. R. V., Ward, R. A., Mellor, M. J., Hughes, G., Rahi, A., Jacobs, V. N., Brewer, M. R., Ichihara, E., Sun, J., Jin, H., Ballard, P., Al-Kadhimi, K., … Pao, W. (2014). AZD9291, an irreversible EGFR TKI, overcomes T790M-mediated resistance to EGFR inhibitors in lung cancer. *Cancer Discovery*, *4*(9), 1046–1061. https://doi.org/10.1158/2159-8290.CD-14-0337

Dawson, J. P., Berger, M. B., Lin, C.-C., Schlessinger, J., Lemmon, M. A., & Ferguson, K. M. (2005). Epidermal Growth Factor Receptor Dimerization and Activation Require Ligand-Induced Conformational Changes in the Dimer Interface. *Molecular and Cellular Biology*, *25*(17), 7734–7742. https://doi.org/10.1128/mcb.25.17.7734-7742.2005

DeLeon-Pennell, K. Y., Barker, T. H., & Lindsey, M. L. (2020). Fibroblasts: The arbiters of extracellular matrix remodeling. In *Matrix Biology* (Vols. 91–92, pp. 1–7). Elsevier B.V. https://doi.org/10.1016/j.matbio.2020.05.006

Desai, S. S., Tung, J. C., Zhou, V. X., Grenert, J. P., Malato, Y., Rezvani, M., Español-Suñer, R., Willenbring, H., Weaver, V. M., & Chang, T. T. (2016). Physiological ranges of matrix rigidity modulate primary mouse hepatocyte function in part through hepatocyte nuclear factor 4 alpha. *Hepatology*, *64*(1), 261–275. https://doi.org/10.1002/hep.28450

Desilets, A., Repetto, M., Yang, S. R., & Drilon, A. (2025). Targeting ROS1 rearrangements in non–small cell lung cancer: Current insights and future directions. In *Cancer* (Vol. 131, Number S1). John Wiley and Sons Inc. https://doi.org/10.1002/cncr.35784

Dhanyamraju, P. K., Schell, T. D., Amin, S., & Robertson, G. P. (2022). Drug-Tolerant Persister Cells in Cancer Therapy Resistance. In *Cancer Research* (Vol. 82, Number 14, pp. 2503–2514). American Association for Cancer Research Inc. https://doi.org/10.1158/0008-5472.CAN-21-3844

Di Marco, M. V., & Voena, C. (2022). Review: biological implications of oncogenic rearrangements in non-small cell lung cancer. In *Precision Cancer Medicine* (Vol. 5). AME Publishing Company. https://doi.org/10.21037/pcm-22-7

Dzobo, K., & Dandara, C. (2023). The Extracellular Matrix: Its Composition, Function, Remodeling, and Role in Tumorigenesis. In *Biomimetics* (Vol. 8, Number 2). MDPI. https://doi.org/10.3390/biomimetics8020146

Egeblad, M., Rasch, M. G., & Weaver, V. M. (2010). Dynamic interplay between the collagen scaffold and tumor evolution. In *Current Opinion in Cell Biology* (Vol. 22, Number 5, pp. 697–706). https://doi.org/10.1016/j.ceb.2010.08.015

Elosegui-Artola, A., Bazellières, E., Allen, M. D., Andreu, I., Oria, R., Sunyer, R., Gomm, J. J., Marshall, J. F., Jones, J. L., Trepat, X., & Roca-Cusachs, P. (2014). Rigidity sensing and adaptation through regulation of integrin types. *Nature Materials*, *13*(6), 631–637. https://doi.org/10.1038/nmat3960

Endo, H., & Inoue, M. (2019). Dormancy in cancer. In *Cancer Science* (Vol. 110, Number 2, pp. 474–480). Blackwell Publishing Ltd. https://doi.org/10.1111/cas.13917

Farach-Carson, M. C., Wu, D., & França, C. M. (2024). Proteoglycans in mechanobiology of tissues and organs: Normal functions and mechanopathology. *Proteoglycan Research*, *2*(2). https://doi.org/10.1002/pgr2.21

Feng, X., Cao, F., Wu, X., Xie, W., Wang, P., & Jiang, H. (2024). Targeting extracellular matrix stiffness for cancer therapy. In *Frontiers in Immunology* (Vol. 15). Frontiers Media SA. https://doi.org/10.3389/fimmu.2024.1467602

Ferguson, K. M. (2008). Structure-based view of epidermal growth factor receptor regulation. In *Annual Review of Biophysics* (Vol. 37, pp. 353–373). https://doi.org/10.1146/annurev.biophys.37.032807.125829

Flanagan, L. A., Ju, Y.-E., Marg, B., Osterfield, M., & Janmey, P. A. (n.d.). *Neurite branching on deformable substrates*.

Friedlaender, A., Perol, M., Banna, G. L., Parikh, K., & Addeo, A. (2024). Oncogenic alterations in advanced NSCLC: a molecular super-highway. In *Biomarker Research* (Vol. 12, Number 1). BioMed Central Ltd. https://doi.org/10.1186/s40364-024-00566-0

Fukui, T., Yatabe, Y., Kobayashi, Y., Tomizawa, K., Ito, S., Hatooka, S., Matsuo, K., & Mitsudomi, T. (2012). Clinicoradiologic characteristics of patients with lung adenocarcinoma harboring EML4-ALK fusion oncogene. *Lung Cancer*, *77*(2), 319–325. https://doi.org/10.1016/j.lungcan.2012.03.013

Furukawa, R., Inoue, H., Yoneshima, Y., Tsutsumi, H., Iwama, E., Ikematsu, Y., Ando, N., Shiraishi, Y., Ota, K., Tanaka, K., Nakanishi, Y., & Okamoto, I. (2021). Cytotoxic chemotherapeutic agents and the EGFR-TKI osimertinib induce calreticulin exposure in non–small cell lung cancer. *Lung Cancer*, *155*, 144–150. https://doi.org/10.1016/j.lungcan.2021.03.018

Gaggar, A., & Weathington, N. (2016). Bioactive extracellular matrix fragments in lung health and disease. In *Journal of Clinical Investigation* (Vol. 126, Number 9, pp. 3176–3184). American Society for Clinical Investigation. https://doi.org/10.1172/JCI83147

Gazdar, A. F., & Minna, J. D. (2008). Deregulated EGFR signaling during lung cancer progression: Mutations, amplicons, and autocrine loops. In *Cancer Prevention Research* (Vol. 1, Number 3, pp. 156–160). https://doi.org/10.1158/1940-6207.CAPR-08-0080

Guo, G., Gong, K., Wohlfeld, B., Hatanpaa, K. J., Zhao, D., & Habib, A. A. (2015). Ligand-independent EGFR signaling. In *Cancer Research* (Vol. 75, Number 17, pp. 3436–3441). American Association for Cancer Research Inc. https://doi.org/10.1158/0008-5472.CAN-15-0989

He, Q., Liu, J., Cai, X., He, M., Li, C., Liang, H., Cheng, B., Xia, X., Guo, M., Liang, P., Zhong, R., Li, F., Yu, Z., Zhao, Y., Ou, L., Xiong, S., Li, J., Zhang, J., He, J., & Liang, W. (2021). Comparison of first-generation EGFR-TKIs (gefitinib, erlotinib, and icotinib) as adjuvant therapy in resected NSCLC patients with sensitive EGFR mutations. *Translational Lung Cancer Research*, *10*(11), 4120–4129. https://doi.org/10.21037/tlcr-21-649

Hermanson, G. T. (2013). Immobilization of Ligands on Chromatography Supports. In *Bioconjugate Techniques* (pp. 589–740). Elsevier. https://doi.org/10.1016/b978-0-12-382239-0.00015-7

Ho, T. C., Chang, C. C., Chan, H. P., Chung, T. W., Shu, C. W., Chuang, K. P., Duh, T. H., Yang, M. H., & Tyan, Y. C. (2022). Hydrogels: Properties and Applications in Biomedicine. In *Molecules* (Vol. 27, Number 9). MDPI. https://doi.org/10.3390/molecules27092902

Hoffman, E. T., Uhl, F. E., Asarian, L., Deng, B., Becker, C., Uriarte, J. J., Downs, I., Young, B., & Weiss, D. J. (2023). Regional and disease specific human lung extracellular matrix composition. *Biomaterials*, *293*. https://doi.org/10.1016/j.biomaterials.2022.121960

Huang, J. W., Zeng, H., Zhang, Q., Liu, X. Y., & Feng, C. (2025). Advances in the clinical diagnosis of lung cancer using contrast-enhanced ultrasound. In *Frontiers in Medicine* (Vol. 12). Frontiers Media SA. https://doi.org/10.3389/fmed.2025.1543033

Hynes, R. O. (2009). The extracellular matrix: Not just pretty fibrils. In *Science* (Vol. 326, Number 5957, pp. 1216–1219). https://doi.org/10.1126/science.1176009

Irmer, D., Funk, J. O., & Blaukat, A. (2007). EGFR kinase domain mutations–functional impact and relevance for lung cancer therapy. Oncogene, 26(39), 5693-5701. https://doi.org/10.1038/sj.onc.1210383

Ishihara, S., & Haga, H. (2022). Matrix Stiffness Contributes to Cancer Progression by Regulating Transcription Factors. In *Cancers* (Vol. 14, Number 4). MDPI. https://doi.org/10.3390/cancers14041049

Ishihara, S., Yasuda, M., Harada, I., Mizutani, T., Kawabata, K., & Haga, H. (2013). Substrate stiffness regulates temporary NF-κB activation via actomyosin contractions. *Experimental Cell Research*, *319*(19), 2916–2927. https://doi.org/10.1016/j.yexcr.2013.09.018

Ismail, A., Desai, A., & Boumber, Y. (2025). HER2 alterations in non-small cell lung cancer (NSCLC): from biology and testing to advances in treatment modalities. In *Frontiers in Oncology* (Vol. 15). Frontiers Media SA. https://doi.org/10.3389/fonc.2025.1624124

Izumi, M., Costa, D. B., & Kobayashi, S. S. (2024). Targeting of drug-tolerant persister cells as an approach to counter drug resistance in non-small cell lung cancer. In *Lung Cancer* (Vol. 194). Elsevier Ireland Ltd. https://doi.org/10.1016/j.lungcan.2024.107885

Jain, R. K., Martin, J. D., & Stylianopoulos, T. (2014). The role of mechanical forces in tumor growth and therapy. In *Annual Review of Biomedical Engineering* (Vol. 16, pp. 321–346). Annual Reviews Inc. https://doi.org/10.1146/annurev-bioeng-071813-105259

Jiang, Y., Zhang, H., Wang, J., Liu, Y., Luo, T., & Hua, H. (2022). Targeting extracellular matrix stiffness and mechanotransducers to improve cancer therapy. In *Journal of Hematology and Oncology* (Vol. 15, Number 1). BioMed Central Ltd. https://doi.org/10.1186/s13045-022-01252-0

Joyce, J. A., & Pollard, J. W. (2009). Microenvironmental regulation of metastasis. In *Nature Reviews Cancer* (Vol. 9, Number 4, pp. 239–252). https://doi.org/10.1038/nrc2618

Kandow, C. E., Georges, P. C., Janmey, P. A., & Beningo, K. A. (2007). Polyacrylamide Hydrogels for Cell Mechanics: Steps Toward Optimization and Alternative Uses. In *Methods in Cell Biology* (Vol. 83, pp. 29–46). https://doi.org/10.1016/S0091-679X(07)83002-0

Keane, T. J., Horejs, C. M., & Stevens, M. M. (2018). Scarring vs. functional healing: Matrix-based strategies to regulate tissue repair. In *Advanced Drug Delivery Reviews* (Vol. 129, pp. 407–419). Elsevier B.V. https://doi.org/10.1016/j.addr.2018.02.002

Kim, H. R., Lim, S. M., Kim, H. J., Hwang, S. K., Park, J. K., Shin, E., Bae, M. K., Ou, S. H. I., Wang, J., Jewell, S. S., Kang, D. R., Soo, R. A., Haack, H., Kim, J. H., Shim, H. S., & Cho, B. C. (2013). The frequency and impact of ROS1 rearrangement on clinical outcomes in never smokers with lung adenocarcinoma. *Annals of Oncology*, *24*(9), 2364–2370. https://doi.org/10.1093/annonc/mdt220

Kpeglo, D., Hughes, M. D. G., Dougan, L., Haddrick, M., Knowles, M. A., Evans, S. D., & Peyman, S. A. (2022). Modeling the mechanical stiffness of pancreatic ductal adenocarcinoma. *Matrix Biology Plus*, *14*. https://doi.org/10.1016/j.mbplus.2022.100109

Kraning-Rush, C. M., & Reinhart-King, C. A. (2012). Controlling matrix stiffness and topography for the study of tumor cell migration. In *Cell Adhesion and Migration* (Vol. 6, Number 3, pp. 274–279). Taylor and Francis Inc. https://doi.org/10.4161/cam.21076

Lategahn, J., Keul, M., Klövekorn, P., Tumbrink, H. L., Niggenaber, J., Müller, M. P., Hodson, L., Flaßhoff, M., Hardick, J., Grabe, T., Engel, J., Schultz-Fademrecht, C., Baumann, M., Ketzer, J., Mühlenberg, T., Hiller, W., Günther, G., Unger, A., Müller, H., … Rauh, D. (2019). Inhibition of osimertinib-resistant epidermal growth factor receptor EGFR-T790M/C797S. *Chemical Science*, *10*(46), 10789–10801. https://doi.org/10.1039/c9sc03445e

Lee, N. Y., Hazlett, T. L., & Koland, J. G. (2006). Structure and dynamics of the epidermal growth factor receptor C-terminal phosphorylation domain. *Protein Science*, *15*(5), 1142–1152. https://doi.org/10.1110/ps.052045306

Leonetti, A., Sharma, S., Minari, R., Perego, P., Giovannetti, E., & Tiseo, M. (2019). Resistance mechanisms to osimertinib in EGFR-mutated non-small cell lung cancer. In *British Journal of Cancer* (Vol. 121, Number 9, pp. 725–737). Nature Publishing Group. https://doi.org/10.1038/s41416-019-0573-8

Li, A. R., Chitale, D., Riely, G. J., Pao, W., Miller, V. A., Zakowski, M. F., Rusch, V., Kris, M. G., & Ladanyi, M. (2008). Clinical testing experience and relationship to EGFR gene copy number and immunohistochemical expression. *Journal of Molecular Diagnostics*, *10*(3), 242–248. https://doi.org/10.2353/jmoldx.2008.070178

Li, Y., Mao, T., Wang, J., Zheng, H., Hu, Z., Cao, P., Yang, S., Zhu, L., Guo, S., Zhao, X., Tian, Y., Shen, H., & Lin, F. (2023). Toward the next generation EGFR inhibitors: an overview of osimertinib resistance mediated by EGFR mutations in non-small cell lung cancer. In *Cell Communication and Signaling* (Vol. 21, Number 1). BioMed Central Ltd. https://doi.org/10.1186/s12964-023-01082-8

Liang, R., & Song, G. (2023). Matrix stiffness-driven cancer progression and the targeted therapeutic strategy. In *Mechanobiology in Medicine* (Vol. 1, Number 2). Elsevier B.V. https://doi.org/10.1016/j.mbm.2023.100013

Liao, Y. Y., Tsai, C. L., & Huang, H. P. (2025). Optimizing Osimertinib for NSCLC: Targeting Resistance and Exploring Combination Therapeutics. In *Cancers* (Vol. 17, Number 3). Multidisciplinary Digital Publishing Institute (MDPI). https://doi.org/10.3390/cancers17030459

Liu, S., Jiang, A., Tang, F., Duan, M., & Li, B. (2025). Drug-induced tolerant persisters in tumor: mechanism, vulnerability and perspective implication for clinical treatment. In *Molecular Cancer* (Vol. 24, Number 1). BioMed Central Ltd. https://doi.org/10.1186/s12943-025-02323-9

Lu, P., Takai, K., Weaver, V. M., & Werb, Z. (2011). Extracellular Matrix degradation and remodeling in development and disease. *Cold Spring Harbor Perspectives in Biology*, *3*(12). https://doi.org/10.1101/cshperspect.a005058

Marinelli, D., Siringo, M., Metro, G., Ricciuti, B., & Gelibter, A. J. (2022). Non-small-cell lung cancer: how to manage ALK-, ROS1- And NTRK-rearranged disease. In *Drugs in Context* (Vol. 11). Bioexcel Publishing LTD. https://doi.org/10.7573/dic.2022-3-1

Masuzawa, K., Yasuda, H., Hamamoto, J., Nukaga, S., Hirano, T., Kawada, I., Naoki, K., Soejima, K., & Betsuyaku, T. (n.d.). *Characterization of the efficacies of osimertinib and nazartinib against cells expressing clinically relevant epidermal growth factor receptor mutations*. Retrieved www.impactjournals.com/oncotarget

Mayer, C., Ofek, E., Fridrich, D. E., Molchanov, Y., Yacobi, R., Gazy, I., Hayun, I., Zalach, J., Paz-Yaacov, N., & Barshack, I. (2022). Direct identification of ALK and ROS1 fusions in non-small cell lung cancer from hematoxylin and eosin-stained slides using deep learning algorithms. *Modern Pathology*, *35*(12), 1882–1887. https://doi.org/10.1038/s41379-022-01141-4

McCoach, C. E., & Jimeno, A. (2016). Osimertinib, a third-generation tyrosine kinase inhibitor targeting non-small cell lung cancer with EGFR T790M mutations. *Drugs of Today (Barcelona, Spain: 1998)*, *52*(10), 561-568.

Melosky, B., Kambartel, K., Häntschel, M., Bennetts, M., Nickens, D. J., Brinkmann, J., Kayser, A., Moran, M., & Cappuzzo, F. (2022). Worldwide Prevalence of Epidermal Growth Factor Receptor Mutations in Non-Small Cell Lung Cancer: A Meta-Analysis. In *Molecular Diagnosis and Therapy* (Vol. 26, Number 1, pp. 7–18). Adis. https://doi.org/10.1007/s40291-021-00563-1

Mendoza, M. C., Er, E. E., & Blenis, J. (2011). The Ras-ERK and PI3K-mTOR pathways: Cross-talk and compensation. In *Trends in Biochemical Sciences* (Vol. 36, Number 6, pp. 320–328). https://doi.org/10.1016/j.tibs.2011.03.006

Mulkidjan, R. S., Saitova, E. S., Preobrazhenskaya, E. V., Asadulaeva, K. A., Bubnov, M. G., Otradnova, E. A., Terina, D. M., Shulga, S. S., Martynenko, D. E., Semina, M. V., Belogubova, E. V., Tiurin, V. I., Amankwah, P. S., Martianov, A. S., & Imyanitov, E. N. (2023). ALK, ROS1, RET and NTRK1–3 Gene Fusions in Colorectal and Non-Colorectal Microsatellite-Unstable Cancers. *International Journal of Molecular Sciences*, *24*(17). https://doi.org/10.3390/ijms241713610

Najafi, M., Goradel, N. H., Farhood, B., Salehi, E., Solhjoo, S., Toolee, H., Kharazinejad, E., & Mortezaee, K. (2019). Tumor microenvironment: Interactions and therapy. In *Journal of Cellular Physiology* (Vol. 234, Number 5, pp. 5700–5721). Wiley-Liss Inc. https://doi.org/10.1002/jcp.27425

Nussinov, R., Tsai, C. J., & Jang, H. (2016). Independent and core pathways in oncogenic KRAS signaling. In *Expert Review of Proteomics* (Vol. 13, Number 8, pp. 711–716). Taylor and Francis Ltd. https://doi.org/10.1080/14789450.2016.1209417

Onursal, C., Dick, E., Angelidis, I., Schiller, H. B., & Staab-Weijnitz, C. A. (2021). Collagen Biosynthesis, Processing, and Maturation in Lung Ageing. In *Frontiers in Medicine* (Vol. 8). Frontiers Media S.A. https://doi.org/10.3389/fmed.2021.593874

Pan, C., Zheng, L., & Wang, J. (2025). Cancer associated fibroblasts in tumors: focusing on solid tumors and hematological malignancies. In *Frontiers in Oncology* (Vol. 15). Frontiers Media SA. https://doi.org/10.3389/fonc.2025.1596947

Park, Y., Lee, D., Lee, J. E., Park, H. S., Jung, S. S., Park, D., Kang, D. H., Lee, S. I., Woo, S. D., & Chung, C. (2024). The Matrix Stiffness Coordinates the Cell Proliferation and PD-L1 Expression via YAP in Lung Adenocarcinoma. *Cancers*, *16*(3). https://doi.org/10.3390/cancers16030598

Parker, A. L., & Cox, T. R. (2020). The Role of the ECM in Lung Cancer Dormancy and Outgrowth. In *Frontiers in Oncology* (Vol. 10). Frontiers Media S.A. https://doi.org/10.3389/fonc.2020.01766

Pérez-Calixto, D., Amat-Shapiro, S., Zamarrón-Hernández, D., Vázquez-Victorio, G., Puech, P. H., & Hautefeuille, M. (2021). Determination by relaxation tests of the mechanical properties of soft polyacrylamide gels made for mechanobiology studies. *Polymers*, *13*(4), 1–28. https://doi.org/10.3390/polym13040629

Peters, S., & Zimmermann, S. (2014). Targeted therapy in NSCLC driven by HER2 insertions. In *Translational Lung Cancer Research* (Vol. 3, Number 2, pp. 84–88). AME Publishing Company. https://doi.org/10.3978/j.issn.2218-6751.2014.02.06

Petrik, J., Campbell, N. E., Kellenberger, L., Greenaway, J., Moorehead, R. A., & Linnerth-Petrik, N. M. (2010). Extracellular matrix proteins and tumor angiogenesis. In *Journal of Oncology*. https://doi.org/10.1155/2010/586905

Pineda-Hernandez, A., Castilla-Casadiego, D. A., Morton, L. D., Giordano-Nguyen, S. A., Halwachs, K. N., & Rosales, A. M. (2025). Tunable hydrogel networks by varying secondary structures of hydrophilic peptoids provide viable 3D cell culture platforms for hMSCs. *Biomaterials Science*, *13*(12), 3380–3394. https://doi.org/10.1039/d5bm00433k

Piotrowska, Z., Isozaki, H., Lennerz, J. K., Gainor, J. F., Lennes, I. T., Zhu, V. W., Marcoux, N., Banwait, M. K., Digumarthy, S. R., Su, W., Yoda, S., Riley, A. K., Nangia, V., Lin, J. J., Nagy, R. J., Lanman, R. B., Dias-Santagata, D., Mino-Kenudson, M., Iafrate, A. J., … Sequist, L. V. (2018). Landscape of acquired resistance to osimertinib in EGFR-mutant NSCLC and clinical validation of combined EGFR and RET inhibition with osimertinib and

BLU-667 for acquired RET fusion. *Cancer Discovery*, *8*(12), 1529–1539. https://doi.org/10.1158/2159-8290.CD-18-1022

Pisano, C., Witel, G., De Filippis, M., Listì, A., Napoli, F., Righi, L., Novello, S., & Bironzo, P. (2022). Moving through rare lung cancer histologies: a narrative review on diagnosis and treatment of selected infrequent entities. In *Precision Cancer Medicine* (Vol. 5). AME Publishing Company. https://doi.org/10.21037/pcm-22-4

Pompili, S., Latella, G., Gaudio, E., Sferra, R., & Vetuschi, A. (2021). The Charming World of the Extracellular Matrix: A Dynamic and Protective Network of the Intestinal Wall. In *Frontiers in Medicine* (Vol. 8). Frontiers Media S.A. https://doi.org/10.3389/fmed.2021.610189

Popova, N. V., & Jücker, M. (2022). The Functional Role of Extracellular Matrix Proteins in Cancer. In *Cancers* (Vol. 14, Number 1). MDPI. https://doi.org/10.3390/cancers14010238

Purba, E. R., Saita, E. I., & Maruyama, I. N. (2017). Activation of the EGF receptor by ligand binding and oncogenic mutations: The “rotation model.” In *Cells* (Vol. 6, Number 2). MDPI. https://doi.org/10.3390/cells6020013

Ricciuti, B., & Chiari, R. (2018). First line osimertinib for the treatment of patients with advanced EGFR-mutant NSCLC. In *Translational Lung Cancer Research* (Vol. 7, pp. S127–S130). AME Publishing Company. https://doi.org/10.21037/tlcr.2018.03.06

Riely, G. J., Wood, D. E., Ettinger, D. S., Aisner, D. L., Akerley, W., Bauman, J. R., Bharat, A., Bruno, D. S., Chang, J. Y., Chirieac, L. R., DeCamp, M., Desai, A. P., Dilling, T. J., Dowell, J., Durm, G. A., Gettinger, S., Grotz, T. E., Gubens, M. A., Juloori, A., … Hang, L. (2024). Non–Small Cell Lung Cancer, Version 4.2024. *JNCCN Journal of the National Comprehensive Cancer Network*, *22*(4), 249–274. https://doi.org/10.6004/jnccn.2204.0023

Ross, T. D., Coon, B. G., Yun, S., Baeyens, N., Tanaka, K., Ouyang, M., & Schwartz, M. A. (2013). Integrins in mechanotransduction. In *Current Opinion in Cell Biology* (Vol. 25, Number 5, pp. 613–618). https://doi.org/10.1016/j.ceb.2013.05.006

Safaei, S., Sajed, R., Shariftabrizi, A., Dorafshan, S., Saeednejad Zanjani, L., Dehghan Manshadi, M., Madjd, Z., & Ghods, R. (2023). Tumor matrix stiffness provides fertile soil for cancer stem cells. In *Cancer Cell International* (Vol. 23, Number 1). BioMed Central Ltd. https://doi.org/10.1186/s12935-023-02992-w

Sequist, L. V., Waltman, B. A., Dias-Santagata, D., Digumarthy, S., Turke, A. B., Fidias, P., Bergethon, K., Shaw, A. T., Gettinger, S., Cosper, A. K., Akhavanfard, S., Heist, R. S., Temel, J., Christensen, J. G., Wain, J. C., Lynch, T. J., Vernovsky, K., Mark, E. J., Lanuti, M., … Engelman, J. A. (2011). Genotypic and histological evolution of lung cancers

acquiring resistance to EGFR inhibitors. *Science Translational Medicine*, *3*(75). https://doi.org/10.1126/scitranslmed.3002003

Siegel, R. L., Giaquinto, A. N., & Jemal, A. (2024). Cancer statistics, 2024. *CA: A Cancer Journal for Clinicians*, *74*(1), 12–49. https://doi.org/10.3322/caac.21820

Siegel, R. L., Miller, K. D., & Jemal, A. (2020). Cancer statistics, 2020. *CA: A Cancer Journal for Clinicians*, *70*(1), 7–30. https://doi.org/10.3322/caac.21590

Skoulidis, F., Byers, L. A., Diao, L., Papadimitrakopoulou, V. A., Tong, P., Izzo, J., Behrens, C., Kadara, H., Parra, E. R., Canales, J. R., Zhang, J., Giri, U., Gudikote, J., Cortez, M. A., Yang, C., Fan, Y., Peyton, M., Girard, L., Coombes, K. R., … Heymach, J. V. (2015). Co-occurring genomic alterations define major subsets of KRAS-mutant lung adenocarcinoma with distinct biology, immune profiles, and therapeutic vulnerabilities. *Cancer Discovery*, *5*(8), 861–878. https://doi.org/10.1158/2159-8290.CD-14-1236

Skoulidis, F., & Heymach, J. V. (2019). Co-occurring genomic alterations in non-small-cell lung cancer biology and therapy. In *Nature Reviews Cancer* (Vol. 19, Number 9, pp. 495–509). Nature Publishing Group. https://doi.org/10.1038/s41568-019-0179-8

Su, J., Zhong, W., Zhang, X., Huang, Y., Yan, H., Yang, J., Dong, Z., Xie, Z., Zhou, Q., Huang, X., Lu, D., Yan, W., & Wu, Y.-L. (2017). *Molecular characteristics and clinical outcomes of EGFR exon 19 indel subtypes to EGFR TKIs in NSCLC patients*. www.impactjournals.com/oncotarget

Subramani, R., Izquierdo-Alvarez, A., Bhattacharya, P., Meerts, M., Moldenaers, P., Ramon, H., & Van Oosterwyck, H. (2020). The Influence of Swelling on Elastic Properties of Polyacrylamide Hydrogels. *Frontiers in Materials*, *7*. https://doi.org/10.3389/fmats.2020.00212

Sutto, L., & Gervasio, F. L. (2013). Effects of oncogenic mutations on the conformational free-energy landscape of EGFR kinase. *Proceedings of the National Academy of Sciences of the United States of America*, *110*(26), 10616–10621. https://doi.org/10.1073/pnas.1221953110

Syed, S., Schober, J., Blanco, A., & Zustiak, S. P. (2017). Morphological adaptations in breast cancer cells as a function of prolonged passaging on compliant substrates. *PLoS ONE*, *12*(11). https://doi.org/10.1371/journal.pone.0187853

Takamochi, K., Oh, S., & Suzuki, K. (2013). Differences in EGFR and KRAS mutation spectra in lung adenocarcinoma of never and heavy smokers. *Oncology Letters*, *6*(5), 1207–1212. https://doi.org/10.3892/ol.2013.1551

Tang, F. H., Wong, H. Y. T., Tsang, P. S. W., Yau, M., Tam, S. Y., Law, L., Yau, K., Wong, J., Farah, F. H. M., & Wong, J. (2025). Recent advancements in lung cancer research: a

narrative review. In *Translational Lung Cancer Research* (Vol. 14, Number 3, pp. 975–990). AME Publishing Company. https://doi.org/10.21037/tlcr-24-979

Thai, A. A., Solomon, B. J., Sequist, L. V., Gainor, J. F., & Heist, R. S. (2021). Lung cancer. In *The Lancet* (Vol. 398, Number 10299, pp. 535–554). Elsevier B.V. https://doi.org/10.1016/S0140-6736(21)00312-3

Tse, J. R., & Engler, A. J. (2010). Preparation of hydrogel substrates with tunable mechanical properties. In *Current Protocols in Cell Biology* (Number SUPPL. 47). https://doi.org/10.1002/0471143030.cb1016s47

Uribe, M. L., Marrocco, I., & Yarden, Y. (2021). *cancers EGFR in Cancer: Signaling Mechanisms, Drugs, and Acquired Resistance*. https://doi.org/10.3390/cancers

Vieira, S., Silva-Correia, J., Reis, R. L., & Oliveira, J. M. (2022). Engineering Hydrogels for Modulation of Material-Cell Interactions. In *Macromolecular Bioscience* (Vol. 22, Number 10). John Wiley and Sons Inc. https://doi.org/10.1002/mabi.202200091

Vignaud, T., Ennomani, H., & Théry, M. (2014). Polyacrylamide Hydrogel Micropatterning. In *Methods in Cell Biology* (Vol. 120, pp. 93–116). Academic Press Inc. https://doi.org/10.1016/B978-0-12-417136-7.00006-9

Wagner, M. J., Stacey, M. M., Liu, B. A., & Pawson, T. (2013). Molecular mechanisms of SH2- and PTB-Domain-containing proteins in receptor tyrosine kinase signaling. *Cold Spring Harbor Perspectives in Biology*, *5*(12). https://doi.org/10.1101/cshperspect.a008987

Wang, J., Guo, C., Wang, J., Zhang, X., Qi, J., Huang, X., Hu, Z., Wang, H., & Hong, B. (2025). Tumor Mutation Signature Reveals the Risk Factors of Lung Adenocarcinoma with EGFR or KRAS Mutation. *Cancer Control*, *32*. https://doi.org/10.1177/10732748241307363

Wee, P., & Wang, Z. (2017). Epidermal growth factor receptor cell proliferation signaling pathways. In *Cancers* (Vol. 9, Number 5). MDPI AG. https://doi.org/10.3390/cancers9050052

Wei, J., Yao, J., Yan, M., Xie, Y., Liu, P., Mao, Y., & Li, X. (2022). The role of matrix stiffness in cancer stromal cell fate and targeting therapeutic strategies. In *Acta Biomaterialia* (Vol. 150, pp. 34–47). Acta Materialia Inc. https://doi.org/10.1016/j.actbio.2022.08.005

Wells, R. G. (2013). Tissue mechanics and fibrosis. In *Biochimica et Biophysica Acta - Molecular Basis of Disease* (Vol. 1832, Number 7, pp. 884–890). Elsevier. https://doi.org/10.1016/j.bbadis.2013.02.007

Wolfel, A., Jin, M., & Paez, J. I. (2022). Current strategies for ligand bioconjugation to poly(acrylamide) gels for 2D cell culture: Balancing chemo-selectivity, biofunctionality, and user-friendliness. In *Frontiers in Chemistry* (Vol. 10). Frontiers Media S.A. https://doi.org/10.3389/fchem.2022.1012443

Worthen, C. A., Rittié, L., & Fisher, G. J. (2017). Mechanical deformation of cultured cells with hydrogels. In *Methods in Molecular Biology* (Vol. 1627, pp. 245–251). Humana Press Inc. https://doi.org/10.1007/978-1-4939-7113-8_17

Wu, X., Zhang, J., & Yoshida, Y. (2025). Disentangling the effects of various risk factors and trends in lung cancer mortality. *Scientific Reports*, *15*(1). https://doi.org/10.1038/s41598-025-92373-2

Yamaoka, T., Ohba, M., & Ohmori, T. (2017). Molecular-targeted therapies for epidermal growth factor receptor and its resistance mechanismse. In *International Journal of Molecular Sciences* (Vol. 18, Number 11). MDPI AG. https://doi.org/10.3390/ijms18112420

Yan, N., Guo, S., Zhang, H., Zhang, Z., Shen, S., & Li, X. (2022). BRAF-Mutated Non-Small Cell Lung Cancer: Current Treatment Status and Future Perspective. In *Frontiers in Oncology* (Vol. 12). Frontiers Media S.A. https://doi.org/10.3389/fonc.2022.863043

Yue, B. (2014). Biology of the extracellular matrix: An overview. In *Journal of Glaucoma* (Vol. 23, Number 8, pp. S20–S23). Lippincott Williams and Wilkins. https://doi.org/10.1097/IJG.0000000000000108

Yun, C.-H., Boggon, T. J., Li, Y., Woo, M. S., Greulich, H., Meyerson, M., Eck, M. J., & Eck, M. (2007). Structures of lung cancer-derived EGFR mutants and inhibitor complexes: Mechanism of activation and insights into differential inhibitor sensitivity. In *Cancer Cell* (Vol. 11, Number 3).

Zaffryar-Eilot, S., & Hasson, P. (2022). Lysyl Oxidases: Orchestrators of Cellular Behavior and ECM Remodeling and Homeostasis. In *International Journal of Molecular Sciences* (Vol. 23, Number 19). MDPI. https://doi.org/10.3390/ijms231911378

Zappa, C., & Mousa, S. A. (2016). Non-small cell lung cancer: Current treatment and future advances. *Translational Lung Cancer Research*, *5*(3), 288–300. https://doi.org/10.21037/tlcr.2016.06.07

Zbek, S. O. ¨, Balasubramanian, P. G., Chiquet-Ehrismann, R., Tucker, R. P., & Adams, J. C. (2010). PERSPECTIVES The Evolution of Extracellular Matrix. *Molecular Biology of the Cell*, *21*, 4300–4305. https://doi.org/10.1091/mbc.E10

Zeng, F., & Harris, R. C. (2014). Epidermal growth factor, from gene organization to bedside. In *Seminars in Cell and Developmental Biology* (Vol. 28, pp. 2–11). Elsevier Ltd. https://doi.org/10.1016/j.semcdb.2014.01.011

Zhang, H. (2016). Osimertinib making a breakthrough in lung cancer targeted therapy. In *OncoTargets and Therapy* (Vol. 9, pp. 5489–5493). Dove Medical Press Ltd. https://doi.org/10.2147/OTT.S114722

Zhang, M., & Zhang, B. (2025). Extracellular matrix stiffness: mechanisms in tumor progression and therapeutic potential in cancer. In *Experimental Hematology and Oncology* (Vol. 14, Number 1). BioMed Central Ltd. https://doi.org/10.1186/s40164-025-00647-2

Zhang, T., Qu, R., Chan, S., Lai, M., Tong, L., Feng, F., Chen, H., Song, T., Song, P., Bai, G., Liu, Y., Wang, Y., Li, Y., Su, Y., Shen, Y., Sun, Y., Chen, Y., Geng, M., Ding, K., … Xie, H. (2020). Discovery of a novel third-generation EGFR inhibitor and identification of a potential combination strategy to overcome resistance. *Molecular Cancer*, *19*(1). https://doi.org/10.1186/s12943-020-01202-9

Zhang, Y., Vaccarella, S., Morgan, E., Li, M., Etxeberria, J., Chokunonga, E., Manraj, S. S., Kamate, B., Omonisi, A., & Bray, F. (2023). Global variations in lung cancer incidence by histological subtype in 2020: a population-based study. *The Lancet Oncology*, *24*(11), 1206–1218. https://doi.org/10.1016/S1470-2045(23)00444-8

Zhang, Z., Stiegler, A. L., Boggon, T. J., Kobayashi, S., & Halmos, B. (2010). EGFR-mutated lung cancer: a paradigm of molecular oncology. In *Oncotarget* (Vol. 1, Number 7). www.impactjournals.com/oncotarget497

Zhang, Z., Yang, S., & Wang, Q. (2019). Impact of MET alterations on targeted therapy with EGFR-tyrosine kinase inhibitors for EGFR-mutant lung cancer. In *Biomarker Research* (Vol. 7, Number 1). BioMed Central Ltd. https://doi.org/10.1186/s40364-019-0179-6

Zhong, J. (2016). RAS and downstream RAF-MEK and PI3K-AKT signaling in neuronal development, function and dysfunction. In *Biological Chemistry* (Vol. 397, Number 3, pp. 215–222). Walter de Gruyter GmbH. https://doi.org/10.1515/hsz-2015-0270

Zhou, Y., Horowitz, J. C., Naba, A., Ambalavanan, N., Atabai, K., Balestrini, J., Bitterman, P. B., Corley, R. A., Ding, B. Sen, Engler, A. J., Hansen, K. C., Hagood, J. S., Kheradmand, F., Lin, Q. S., Neptune, E., Niklason, L., Ortiz, L. A., Parks, W. C., Tschumperlin, D. J., … Thannickal, V. J. (2018). Extracellular matrix in lung development, homeostasis and disease. In *Matrix Biology* (Vol. 73, pp. 77–104). Elsevier B.V. https://doi.org/10.1016/j.matbio.2018.03.005